

PM/98-34  
 THES-TP 98/08  
 hep-ph/9811413  
 November 1998

# Tests of Higgs Boson Couplings at a $\mu^+\mu^-$ Collider<sup>†</sup>

G.J. Gounaris<sup>a</sup>, F.M. Renard<sup>b</sup>

<sup>a</sup>Department of Theoretical Physics, University of Thessaloniki,  
 Gr-54006, Thessaloniki, Greece.

<sup>b</sup>Physique Mathématique et Théorique, UMR 5825  
 Université Montpellier II, F-34095 Montpellier Cedex 5.

## Abstract

We investigate the potential of a muon collider for testing the Higgs boson couplings. We consider the case of a light (less than 160  $GeV$ ) Higgs boson and we study the possible non standard couplings induced by  $dim = 6$   $SU(3) \times SU(2) \times U(1)$  gauge invariant operators satisfying the constraints imposed by the present and future LHC and LC colliders. For each operator we give the minimal value of the  $\mu^+\mu^-$  integrated luminosity which would allow a muon collider ( $\mu C$ ) to improve these constraints, on the basis of measurements of the Higgs branching ratios and total width. Depending on the operator and the Higgs mass, this minimal  $\mu C$  luminosity lies between 0.1  $fb^{-1}$  and 100  $fb^{-1}$ .

PACS: 12.15.-y, 12.60.Fr, 14.60.Ef, 14.80.Cp

---

<sup>†</sup>Partially supported by the EC contract CHRX-CT94-0579, and by the NATO grant CRG 971470.

# 1 Introduction

One of the main goals of a future  $\mu^+\mu^-$  collider ( $\mu C$ ), is to provide a Higgs boson factory, [1]. The aim of the present paper is to establish the potential of a  $\mu^+\mu^-$  collider for testing the Higgs boson couplings with a high accuracy. It is assumed that only a single light (*i.e.*  $m_H \lesssim 160$  GeV) standard-like Higgs boson exists, whose total width  $\Gamma_H$  is thus sufficiently small, so that the peak in  $\mu^+\mu^- \rightarrow H$  is enhanced and a large number of events is produced.

The first milestone of this study (Step 1) is the comparison of the measurements of the Higgs decay branching ratios at a  $\mu^+\mu^-$  collider and at an  $e^+e^-$  linear collider (LC). Assuming that the Higgs particle is produced through the process  $\mu^+\mu^- \rightarrow H$  on the one hand, and on the other hand through the process  $e^+e^- \rightarrow HZ$  at LC, we compute the value (versus  $m_H$ ) of the integrated luminosity  $\bar{L}(\mu\mu)$  needed in order for the  $\mu^+\mu^-$  collider to improve the LC measurement done using a luminosity  $\bar{L}(ee)$ .

Provided that this first requirement is satisfied, we go to the second step and quantify, in a gauge invariant way, the meaning of *testing the Higgs boson couplings*. For this purpose we add to the Standard Model (SM) lagrangian  $\mathcal{L}_{SM}$ , a set of new physics (NP) terms associated to a high scale,  $\Lambda$ , lying in the several TeV range. These NP terms are expressed in terms of  $dim = 6$   $SU(3) \times SU(2) \times U(1)$  gauge invariant operators  $\mathcal{O}_i$  involving only SM fields (including the Higgs boson) and contributing with corresponding coupling constants  $g_{eff}^i$ . The contributions of each of these  $dim = 6$  operators on the partial decay widths  $\Gamma(H \rightarrow F)$  are computed, which are then used to derive the constraints on the corresponding coupling constants  $g_{eff}^i$ , that are expected to be established from searches at the various colliders (LEP, SLC, TEVATRON, LHC, LC), anticipated to run before the  $\mu C$ . Given these constraints, the observability of NP at  $\mu C$  depends of course on the integrated luminosity  $\bar{L}(\mu\mu)$  that will be accumulated. Thus, in this second step, we establish the minimum luminosity  $\bar{L}(\mu\mu)$  required in order for the muon-muon Collider to either improve the constraints attainable from the LEP, SLC, TEVATRON, LHC or LC colliders expected to run earlier in time, or possibly even to observe some NP.

Finally, in a third step we discuss what further improvements could be gained by an accurate measurement of the total Higgs width  $\Gamma_H$ .

The contents of the paper is the following:  
Section 2 is devoted to the standard description of Higgs boson formation in  $\mu^+\mu^-$  collisions. We give the SM values of the total and partial widths, as well as the branching ratios of the Higgs particle versus the Higgs mass. For each final state we add the background coming from processes not passing through the Higgs and apply some detection coefficients; like *e.g.* the b efficiency and the  $W, Z$  leptonic branching ratios. This determines the accuracy at which these branching ratios can be measured in a muon Collider. We can then make a fair comparison with the accuracies attainable at LC through the process  $e^+e^- \rightarrow HZ$  and a given  $\bar{L}(ee)$ .

In Section 3 we list the various  $dim = 6$  operators that can affect the Higgs couplings. Their effects on the Higgs decay widths are described in Section 4, with all analytic expressions given in Appendix A. We also give the constraints on the various coupling

constants expected from studies that should be realized at the various colliders before the start of the  $\mu^+\mu^-$  one. In Section 5 we present a study of the Higgs branching ratios for each operator, and give the value of the  $\mu^+\mu^-$  luminosity required to improve the previous constraints. In Section 6 we study what further improvement could be gained by the additional measurement of the Higgs total width. Finally we summarize the implications for the search of new physics in Section 7.

## 2 The Higgs resonance at a $\mu^+\mu^-$ collider

The integrated cross section of the process  $\mu^+\mu^- \rightarrow H \rightarrow F$  is basically given by the Breit-Wigner expression for unpolarized  $\mu^\pm$  beams

$$\sigma(\mu^+\mu^- \rightarrow H \rightarrow F) = \frac{4\pi m_H^2 \Gamma_{H \rightarrow \mu^+\mu^-}(s) \Gamma_{H \rightarrow F}(s)}{s[(s - M_H^2)^2 + m_H^2 \Gamma_H^2(s)]} . \quad (1)$$

We assume a gaussian  $\mu^\pm$  beam energy resolution  $\Delta \sim 2 \text{ MeV}(\sqrt{s}/100 \text{ GeV})$  and ignore initial state radiation effects. For  $\Delta \lesssim \Gamma_H$ , the peak cross section for the production of channel  $F$  at  $\sqrt{s} = m_H$  is given, [1], by

$$\bar{\sigma}(\mu^+\mu^- \rightarrow H \rightarrow F) \simeq \frac{4\pi}{m_H^2} \frac{B(H \rightarrow \mu^+\mu^-) B(H \rightarrow F)}{\left[1 + \frac{8\Delta^2}{\pi\Gamma_H^2}\right]^{\frac{1}{2}}} , \quad (2)$$

while the total cross section obtained by summing over all final states  $F$  is

$$\bar{\sigma}_H \equiv \sum_F \bar{\sigma}(\mu^+\mu^- \rightarrow H \rightarrow (F)) \simeq \frac{4\pi}{m_H^2} \frac{B(H \rightarrow \mu^+\mu^-)}{\left[1 + \frac{8\Delta^2}{\pi\Gamma_H^2}\right]^{\frac{1}{2}}} . \quad (3)$$

The use of (2) and (3) determines the Higgs branching ratios, without requiring an accurate knowledge of the total width  $\Gamma_H$ . Using this and the SM predictions for the partial widths given in Appendix A, we estimate below the attainable accuracy in terms of the  $\mu C$  integrated luminosity  $\bar{L}(\mu\mu)$ .

### 2.1 The total and partial widths of the Higgs particle.

The main channels to study Higgs decay are:

- $f\bar{f}$ , with  $f$  being a  $\mu$  or  $\tau$  lepton, or a  $c$  or  $b$  quark. The various partial widths are expressed in terms of the fermion mass  $m_f$  and couplings. In the case of quarks the running mass  $m_q(m_H)$  is used in agreement with [2].
- $WW^*$  and  $ZZ^*$ . For the interesting range of our study  $M_Z \lesssim m_H \lesssim 2M_W$ , we consider the decay modes  $H \rightarrow WW^* \rightarrow Wf\bar{f}$  and  $H \rightarrow ZZ^* \rightarrow Zf\bar{f}$  expressed in terms of  $M_{W,Z}$  and  $(W,Z)f\bar{f}$  couplings.

- $\gamma\gamma$  and  $Z\gamma$ . In SM at the 1 loop level, they are determined through a  $t$ -quark or  $W$  loop.
- $gg$ . In SM they are determined by a  $t$ -quark loop contribution to which further QCD corrections should be applied.

Summing the SM partial widths  $\Gamma(H \rightarrow F)$ , one obtains the total Higgs width

$$\Gamma_H \equiv \sum_F \Gamma(H \rightarrow F) , \quad (4)$$

and the various branching ratios

$$B(H \rightarrow F) = \frac{\Gamma(H \rightarrow F)}{\Gamma_H} . \quad (5)$$

The SM results for the total width and the branching ratios, (constructed from the formulas in the Appendix) are shown in Figs.1,2. The same results are also presented in Table 1 for the case  $m_H = 130 \text{ GeV}$ , for which  $\Gamma_H \simeq 4.67 \text{ MeV}$ .

**Table 1: SM values of partial Higgs widths (MeV) and branching ratios for  $m_H = 130 \text{ GeV}$**

	$\mu^+\mu^-$	$\tau^+\tau^-$	$b\bar{b}$	$c\bar{c}$	$WW^*$	$ZZ^*$	$gg$	$\gamma\gamma$	$Z\gamma$
$\Gamma(H \rightarrow F)$	$0.95 \times 10^{-3}$	0.27	2.43	0.11	1.33	0.16	0.34	0.012	0.010
$B(H \rightarrow F)$	0.00020	0.057	0.52	0.024	0.28	0.035	0.073	0.0026	0.0021

## 2.2 Number of Higgs events, backgrounds and accuracies

The peak value of Higgs production cross section given by (3), is shown in Fig.3. For  $m_H = 130 \text{ GeV}$  it is equal to  $\bar{\sigma}_H \simeq 4. \times 10^4 \text{ fb}$ . Therefore, an integrated luminosity  $\bar{L}(\mu\mu)$  in the range of  $1 \text{ fb}^{-1}$ , leading to a total number of about  $4. \times 10^4$  Higgs events, should allow important high precision tests of the various Higgs decay modes and the related couplings.

However, in order to make a fair estimate of the accuracy at which these tests can be performed, we have to study the backgrounds and apply some detection efficiencies. Thus, as a background to  $\mu^+\mu^- \rightarrow H \rightarrow F$  we consider the  $\mu^+\mu^- \rightarrow F$  annihilation due to process not involving a Higgs exchange in the  $s$ -channel. Namely  $\mu^+\mu^- \rightarrow b\bar{b}$  (due to  $\gamma$  and  $Z$  exchange),  $\mu^+\mu^- \rightarrow WW^*$  ( $\nu_\mu$ ,  $\gamma$  and  $Z$  exchanges),  $\mu^+\mu^- \rightarrow ZZ^*$  ( $\mu$  exchange),  $\mu^+\mu^- \rightarrow \gamma\gamma$  ( $\mu$  exchange),  $\mu^+\mu^- \rightarrow Z\gamma$  ( $\mu$  exchange). Finally, as a background for the gluon-gluon channel  $\mu^+\mu^- \rightarrow H \rightarrow gg$ , we consider the processes  $\mu^+\mu^- \rightarrow q\bar{q}$  ( $q = u, d, c, s$ ) due to  $\gamma$  and  $Z$  exchanges.

For each channel, we also take into account some rough estimate of the detection efficiency  $\epsilon_F$ . Thus for  $WW^*$ ,  $ZZ^*$  and  $Z\gamma$  pair production, we apply a reduction due

to the requirement of at least one leptonic decay; *i.e.* 0.33 for  $WW^*$ , 0.098 for  $ZZ^*$ , and 0.067 for  $Z\gamma$ . This may be somewhat pessimistic and we should keep in mind that some improvement could be obtained by using hadronic  $Z$  modes. For  $b$  quarks we use a detection efficiency of 50%. In the  $\gamma\gamma$  and  $Z\gamma$  channels we also apply an angular cut  $\cos\theta_{cm} < 0.7$ .

The accuracy on  $B(H \rightarrow \mu\mu)$ , according to (3), is obtained from the total number of events  $N_H^{\mu\mu}(tot) \equiv \bar{L}(\mu\mu)\bar{\sigma}_H \sum_F B(H \rightarrow F)\epsilon_F$ . Taking the background into account this gives

$$\delta_B(\mu\mu) = \frac{\sqrt{N_H^{\mu\mu}(tot) + N_{back}^{\mu\mu}}}{N_H^{\mu\mu}(tot)} . \quad (6)$$

For the other final states  $F$ , the relative accuracy at which the branching ratio  $B(H \rightarrow F)$  can be measured is determined by combining quadratically the accuracy on  $B(H \rightarrow \mu\mu)$  with the accuracy at which  $\bar{\sigma}(\mu^+\mu^- \rightarrow H \rightarrow F)$  can be measured. This last one is obtained by adding the number of Higgs signal events due to (2) to the number of background events  $N_{back}(F)$  for the final state  $F$ . We thus write

$$\delta_B(F) = \sqrt{[\delta_B(\mu\mu)]^2 + \frac{N(F) + N_{back}(F)}{[N(F)]^2}} , \quad (7)$$

where  $N(F) = \bar{L}(\mu\mu)\bar{\sigma}_H B(H \rightarrow F)\epsilon_F$ , with  $\epsilon_F$  being the aformentioned detection efficiency. Note that  $\delta_B(F)$  behaves like  $\bar{L}(\mu\mu)^{-\frac{1}{2}}$ .

Thus, for  $m_H = 130 \text{ GeV}$  and  $\bar{L}(\mu\mu) = 1 \text{ fb}^{-1}$ , we get the results shown in Table 2a.

**Table 2a: Accuracies on  $B(H \rightarrow F)$  for  $m_H = 130 \text{ GeV}$**   
 $(\delta_B(F)$  should be multiplied by  $\bar{L}(\mu\mu)^{-\frac{1}{2}}$ , with  $\bar{L}(\mu\mu)$  measured in  $\text{fb}^{-1}$ )

	$\mu^+\mu^-$	$b\bar{b}$	$WW^*$	$ZZ^*$	$gg$	$\gamma\gamma$	$Z\gamma$
$\delta_B(F)$	0.015	0.020	0.022	0.084	0.085	1.2	4.8

### 2.3 Step 1: Comparison with the measurement of Higgs branching ratios at LC.

We next explore how much such a  $\mu^+\mu^-$  collider can improve the knowledge of the Higgs couplings, as compared to what would be possible from other types of colliders expected to run before; *i.e.* LEP, TEVATRON and future ones like LHC and LC.

At LHC a large number of events should be produced but the accuracy is limited by uncertainties concerning the background, the parton distribution functions and the QCD corrections [3]. Nevertheless, LHC will give, (at the time of its operation), the best constraints on the gluonic couplings of the Higgs [3].

Later on, better measurements of the Higgs branching ratios should come from the LC collider, through the process  $e^+e^- \rightarrow HZ$ . So one should first compare the number of Higgs bosons produced in  $\mu^+\mu^- \rightarrow H$  and in  $e^+e^- \rightarrow HZ$ .

The number of Higgs particles to be collected in a LC is determined by the highest value of the  $e^+e^- \rightarrow HZ$  cross section, occurring at an energy slightly above the  $M_Z + m_H$  threshold. Let us call it  $\sigma^{max}(e^+e^- \rightarrow HZ)$ . In order to test the Higgs boson couplings, a precise measurement of the various Higgs branching ratios ( $b\bar{b}$ ,  $WW^*$ ,  $ZZ^*$ ,  $gg$ ,  $Z\gamma$ ,  $\gamma\gamma$ ,  $\mu^+\mu^-$ ) should be done. This requires a careful study of the backgrounds in all  $ZH$  modes, which is beyond the scope of this paper. We take the simple attitude of requiring a clear  $Z$  identification through its  $e^+e^-$ ,  $\mu^+\mu^-$  decay modes and, consequently, of ignoring any background. In Fig.4 we plot the quantity  $\sigma^{max}(e^+e^- \rightarrow HZ)B(Z \rightarrow e^+e^- + \mu^+\mu^-)$ , as a function of  $m_H$  in SM. The corresponding number of Higgs particles produced at LC is constructed through

$$N_H^{LC} = \bar{L}(ee)\sigma^{max}(e^+e^- \rightarrow HZ)B(Z \rightarrow e^+e^- + \mu^+\mu^-) , \quad (8)$$

where  $\bar{L}(ee)$  is the integrated LC luminosity. A  $\mu^+\mu^-$  collider will increase this number provided that, (compare (3, 8))

$$N_H^{\mu\mu} \equiv \bar{L}(\mu\mu)\bar{\sigma}_H > N_H^{LC} , \quad (9)$$

which requires

$$\frac{\bar{L}(\mu\mu)}{\bar{L}(ee)} > \frac{\sigma^{max}(e^+e^- \rightarrow HZ) \times B(Z \rightarrow e^+e^- + \mu^+\mu^-)}{\bar{\sigma}_H} . \quad (10)$$

In Fig.5, the minimum value of  $\bar{L}(\mu\mu)/\bar{L}(ee)$  implied by (10) is plotted for various values of  $m_H$ .

As an example, we note that  $m_H = 130$  GeV, gives  $\sigma^{max}(e^+e^- \rightarrow HZ)B(Z \rightarrow e^+e^- + \mu^+\mu^-) \simeq 14$  fb at  $\sqrt{s} = 250$  GeV. If we then assume  $\bar{L}(ee) \simeq 100$  fb $^{-1}$ , we would expect  $N_H^{LC} \simeq 1.4 \times 10^3$  well identified Higgs events at such an LC. Assuming subsequently (compare (10)) that  $\bar{L}(\mu\mu)/\bar{L}(ee) \simeq 0.35 \times 10^{-3}$ , we conclude that a  $\mu\mu$  collider with a luminosity  $\bar{L}(\mu\mu) \gtrsim 0.035$  fb $^{-1}$  will produce more Higgs bosons than an LC of the above energy and  $\bar{L}(ee)$ .

We now look at each Higgs decay mode specifically. We still consider  $e^+e^- \rightarrow HZ$  applying the leptonic branching ratio 0.067 for  $Z$  identification. For each  $H \rightarrow F$  decay channel we apply the Higgs branching fractions and the aforementioned detection efficiencies  $\epsilon_F$ . We ignore any background, assuming that the requirement of a clear  $Z$  identification is enough. For the  $b\bar{b}$  channel this may be pessimistic as the  $b$  tagging would already reduce strongly the background even if one considers hadronic  $Z$  modes. For the other Higgs decay modes ( $WW^*$ , ...) a clear  $Z$  identification is probably mandatory. This way, the relative accuracy achievable at an LC is obtained as

$$\delta_B^{LC}(F) \gtrsim \sqrt{1/N_H^{LC}(tot) + 1/N_H^{LC}(F)} , \quad (11)$$

where  $N_H^{LC}(F) = N_H^{LC}B(H \rightarrow F)\epsilon_F$  and  $N_H^{LC}(tot) = \sum_F N_H^{LC}(F)$ , (compare (8)). For  $m_H = 130$  GeV and  $\bar{L}(ee) = 100$  fb $^{-1}$ , the results are shown in Table 2b.

**Table 2b: Lower bounds on the accuracies at LC on  $B(H \rightarrow F)$  for  $m_H = 130 \text{ GeV}$  and  $\bar{L}(ee) = 100 \text{ fb}^{-1}$**

	$\mu^+\mu^-$	$b\bar{b}$	$WW^*$	$ZZ^*$	$gg$	$\gamma\gamma$	$Z\gamma$
$\delta_B^{LC}(F)$	1.8	0.06	0.091	0.45	0.12	0.52	2.2

Comparing Table 2a (scaled by  $\bar{L}(\mu\mu)^{-\frac{1}{2}}$ ) with Table 2b, one observes that a  $\mu^+\mu^-$  luminosity of a fraction of  $\text{fb}^{-1}$  would be sufficient in order to improve the expected LC measurements of the Higgs branching ratios for the main decay modes. For the rare modes ( $\gamma\gamma$ ,  $Z\gamma$ ) a somewhat larger integrated luminosity of the order of a few  $\text{fb}^{-1}$ , would be required. For the  $\mu^+\mu^-$  mode the muon collider is obviously superior.

## 2.4 Further steps.

Assuming that this first requirement on  $\bar{L}(\mu\mu)$  is fulfilled, we will develop (Step 2) a detailed study of the Higgs boson couplings on the basis of the measurement of the various branching ratios  $B(H \rightarrow F)$ .

We will compare the accuracies  $\delta_B(F)$  of (7) with possible NP effects, and further explore the required luminosity, so that the muon collider improves the constraints imposed by earlier machines. Thus, we take into account the constraints on the NP parameters coming from all possible sources; namely the processes  $e^+e^- \rightarrow HZ$  and  $e^+e^- \rightarrow H\gamma$ , constraining the  $HZZ$ ,  $HZ\gamma$  and  $H\gamma\gamma$  couplings at an LC [4]; the Higgs production at LHC constraining the  $Hgg$  coupling; and the indirect constraints on Higgs couplings coming from precision measurements at the Z peak and in  $e^+e^- \rightarrow f\bar{f}$ ,  $W^+W^-$  at LC, [5, 6, 7]. Finally, we will also consider the possibility that  $\gamma\gamma$  collisions will be realized at LC through backscattering of laser photons, which should give very good constraints on the  $H\gamma\gamma$  couplings, [8]. This study will be developed in Sect.5 after having presented the NP operators and their constraints in Sect.3 and 4.

Finally, in a third step we will assume, in addition, that the total Higgs width can be accurately measured from the line shape at the  $\mu^+\mu^-$  collider. This will give direct access to the partial widths  $\Gamma(H \rightarrow F)$  and will allow to reach certain NP couplings which are hidden in the branching ratio measurements.

As in the branching ratio case discussed above, we introduce the achievable relative uncertainty on the total Higgs width denoted by  $\bar{\delta}_\Gamma$ , for which we assume the usual dependence on the integrated luminosity, and write it as

$$\bar{\delta}_\Gamma = \frac{\delta_\Gamma}{\sqrt{\bar{L}(\mu\mu)}} , \quad (12)$$

in terms of a coefficient  $\delta_\Gamma$ , that we will keep as a parameter. It seems reasonable to expect  $\delta_\Gamma$  to be of the order of a few percent. For example for  $m_H = 130 \text{ GeV}$ , this is what one should be able to achieve with  $\bar{L}(\mu\mu) = 1 \text{ fb}^{-1}$  implying a few  $10^4$  events. In

such a case  $\delta_\Gamma = 0.01(0.03)$  would imply an uncertainty of  $0.05(0.15) \text{ MeV}$  on the total width of  $4.67 \text{ MeV}$ .

By combining the measurements of the total width and those of the branching ratios, one obtains measurements of each partial width  $\Gamma(H \rightarrow F)$  with a relative accuracy

$$\delta_\Gamma(F) = \sqrt{(\bar{\delta}_\Gamma)^2 + (\delta_B(F))^2} \quad , \quad (13)$$

where  $\delta_B(F)$  have been defined in (7).

The use of these measurements will be presented in Section 6.

### 3 The $\dim = 6$ operators inducing anomalous Higgs couplings

The effective Lagrangian describing anomalous Higgs properties is written as:

$$\mathcal{L}_{NP} = \Sigma_i g_{eff}^i \mathcal{O}_i \quad . \quad (14)$$

We first consider purely bosonic operators. The full list, in the linear realization, has been given in [5, 9, 10]. We retain only those operators which affect the Higgs boson couplings. There are 8 CP-conserving such operators<sup>1</sup>:

$$\mathcal{O}_{\Phi 1} = (D_\mu \Phi^\dagger \Phi)(\Phi^\dagger D^\mu \Phi) \quad , \quad g_{eff}^{\Phi 1} = \frac{f_{\Phi 1}}{\Lambda^2} = \frac{\bar{f}_{\Phi 1}}{v^2} \quad (15)$$

$$\mathcal{O}_{BW} = \frac{1}{2} \Phi^\dagger B_{\mu\nu} \vec{\tau} \cdot \vec{W}^{\mu\nu} \Phi \quad , \quad g_{eff}^{BW} = -\frac{gg' f_{BW}}{2 \Lambda^2} = \frac{\bar{f}_{BW}}{v^2} \quad (16)$$

$$\mathcal{O}_{B\Phi} = i (D_\mu \Phi)^\dagger B^{\mu\nu} (D_\nu \Phi) \quad , \quad g_{eff}^{B\Phi} = \frac{g' f_B}{2 \Lambda^2} = \frac{g' \bar{f}_B}{2 M_W^2} = \frac{g' \alpha_{B\Phi}}{M_W^2} \quad (17)$$

$$\mathcal{O}_{W\Phi} = i (D_\mu \Phi)^\dagger \vec{\tau} \cdot \vec{W}^{\mu\nu} (D_\nu \Phi) \quad , \quad g_{eff}^{W\Phi} = \frac{g f_W}{2 \Lambda^2} = \frac{g \bar{f}_W}{2 M_W^2} = \frac{g \alpha_{W\Phi}}{M_W^2} \quad (18)$$

$$\mathcal{O}_{WW} = (\Phi^\dagger \Phi) \vec{W}^{\mu\nu} \cdot \vec{W}_{\mu\nu} \quad , \quad g_{eff}^{WW} = -\frac{g^2 f_{WW}}{4 \Lambda^2} = \frac{g^2 d_W}{4 M_W^2} \quad (19)$$

$$\mathcal{O}_{BB} = (\Phi^\dagger \Phi) B^{\mu\nu} B_{\mu\nu} \quad , \quad g_{eff}^{BB} = -\frac{g'^2 f_{BB}}{4 \Lambda^2} = \frac{g^2 d_B}{4 M_W^2} \quad (20)$$

$$\mathcal{O}_{\Phi 2} = 4 \partial_\mu (\Phi^\dagger \Phi) \partial^\mu (\Phi^\dagger \Phi) \quad , \quad g_{eff}^{\Phi 2} = \frac{f_{\Phi 2}}{8 \Lambda^2} = \frac{\bar{f}_{\Phi 2}}{v^2} \quad (21)$$

$$\mathcal{O}_{GG} = (\Phi^\dagger \Phi) \vec{G}^{\mu\nu} \cdot \vec{G}_{\mu\nu} \quad , \quad g_{eff}^{GG} = \frac{d_G}{v^2} \quad , \quad (22)$$

---

<sup>1</sup>The contribution of (19, 20, 22) to the gauge kinetic energy is assumed to have been renormalized away.

where

$$\frac{g'}{g} = \frac{s_W}{c_W} \quad , \quad \sqrt{2}G_F \equiv \frac{1}{v^2} \equiv \frac{4M_W^2}{g^2} \quad , \quad (23)$$

and 4 CP-violating ones:

$$\tilde{\mathcal{O}}_{BW} = \frac{1}{2} \Phi^\dagger B_{\mu\nu} \boldsymbol{\tau} \cdot \tilde{\mathbf{W}}^{\mu\nu} \Phi \quad g_{eff}^{WB} = \frac{\tilde{f}_{BW}}{v^2} \quad , \quad (24)$$

$$\tilde{\mathcal{O}}_{WW} = (\Phi^\dagger \Phi) \mathbf{W}^{\mu\nu} \cdot \tilde{\mathbf{W}}_{\mu\nu} \quad g_{eff}^{WW} = \frac{\tilde{d}_W}{v^2} \quad , \quad (25)$$

$$\tilde{\mathcal{O}}_{BB} = (\Phi^\dagger \Phi) B^{\mu\nu} \tilde{B}_{\mu\nu} \quad g_{eff}^{BB} = \frac{\tilde{d}_B}{v^2} \quad , \quad (26)$$

$$\tilde{\mathcal{O}}_{GG} = (\Phi^\dagger \Phi) \mathbf{G}^{\mu\nu} \cdot \tilde{\mathbf{G}}_{\mu\nu} \quad g_{eff}^{GG} = \frac{\tilde{d}_G}{v^2} \quad , \quad (27)$$

(28)

with<sup>2</sup>  $\tilde{V}^{\mu\nu} = \frac{1}{2} \epsilon^{\mu\nu\alpha\beta} (\partial_\alpha V_\beta - \partial_\beta V_\alpha)$ .

We also consider possible modifications of the fermionic couplings of the Higgs boson. A convenient  $dim = 6$  operator for describing anomalous Higgs and heavy quark interactions was introduced in [9]. In the case of the  $b$  quark it reads :

$$\mathcal{O}_{b1} = (\Phi^\dagger \Phi) [(\bar{f}_L \Phi) b_R + \bar{b}_R (\Phi^\dagger f_L)] \quad , \quad g_{eff}^{b1} = \frac{f_{b1}}{\Lambda^2} = \frac{\bar{f}_{b1}}{v^2} \quad (29)$$

where  $f_L$  is the left handed doublet of the third family of quarks. It was especially motivated by the assumption that NP is associated to the origin of mass generation and should reflect in priority in anomalous properties of heavy particles (heavy quarks, massive gauge bosons and Higgs bosons).

In the present work we also generalize the operator  $\mathcal{O}_{b1}$ , as a convenient parametrization of anomalous  $Hff$  couplings for any fermion  $f$ . For example for charged leptons

$$\mathcal{O}_{l1} = (\Phi^\dagger \Phi) [(\bar{l}_L \Phi) l_R + \bar{l}_R (\Phi^\dagger l_L)] \quad , \quad g_{eff}^{l1} = \frac{f_{l1}}{\Lambda^2} = \frac{\bar{f}_{l1}}{v^2} \quad , \quad (30)$$

where  $l_L, l_R$  are the doublet, singlet of a given family of lepton.

## 4 NP effects on the Higgs partial decay widths

We now consider the effect of the  $dim = 6$  operators on the partial decay widths  $\Gamma(H \rightarrow F)$ , by treating each operator separately. All necessary analytic expressions are given in the Appendix. In all results below, we assume  $\bar{L}(ee) = 100 \text{fb}^{-1}$  for the integrated LC luminosity.

---

<sup>2</sup>In (25 - 27), it is understood that instantonic contribution from the baryon number violating electroweak, as well as the QCD instantons, have been subtracted, so that only Higgs interactions are retained.

For each interaction term  $g_{eff}^i \mathcal{O}_i$ , the relative NP effect on a partial width is written as

$$\Gamma(H \rightarrow F) = \Gamma^{SM}(H \rightarrow F)[1 + \delta^{NP,i}(F)] . \quad (31)$$

The NP effect contained in  $\delta^{NP,i}(F)$ , is controlled by the magnitude of the coupling constant  $g_{eff}^i$ . So for each operator, we first collect the constraint on its coupling, expected from searches at the various colliders, that should run before the start of the  $\mu^+\mu^-$  collider. These are then translated to constraints on  $\delta^{NP,i}(F)$ , using the expressions in the Appendix.

## 4.1 CP-conserving bosonic operators

### 4.1.1 $\mathcal{O}_{\Phi 1}$

This is a "non-blind" operator, inducing a direct  $\Delta\rho$  contribution to the strength of the  $Z$  coupling, which in turn implies that it is strongly constrained by existing precision measurements performed by LEP1/SLC, [5] at the  $Z$  peak. In the future, this constraint may be slightly improved by measurements at LEP2 and LC, where it should reach the level [6]

$$\left| \frac{f_{\Phi,1}}{\Lambda^2} \right| \lesssim 0.035 \text{ TeV}^{-2} \quad \text{or} \quad |\bar{f}_{\Phi,1}| \lesssim 0.002 . \quad (32)$$

This operator leads also to a wave function renormalization of the Higgs field which affects all decay modes (compare (A.3)), and to a direct  $HZZ$  effect.

### 4.1.2 $\mathcal{O}_{BW}$

This is also a "non-blind" operator, mainly constrained by the so-called  $\epsilon_3$  or  $S$  parameters, [12, 11]. These tests give the constraints [5, 6]

$$\left| \frac{f_{BW}}{\Lambda^2} \right| \lesssim 0.27 \text{ TeV}^{-2} \quad \text{or} \quad |\bar{f}_{BW}| \lesssim 0.006 . \quad (33)$$

An even more stringent constraint should be obtained if laser backscattering  $\gamma\gamma$  processes are accessible at LC. Through the process  $\gamma\gamma \rightarrow H$  one should get, generalizing the analysis in [8]

$$\left| \frac{f_{BW}}{\Lambda^2} \right| \lesssim 0.17 \text{ TeV}^{-2} \quad \text{or} \quad |\bar{f}_{BW}| \lesssim 0.0012 . \quad (34)$$

$\mathcal{O}_{BW}$  affects directly the  $HZZ$ ,  $HZ\gamma$  and  $H\gamma\gamma$  couplings.

### 4.1.3 $\mathcal{O}_{B\Phi}$ and $\mathcal{O}_{W\Phi}$

These "blind" operators induce anomalous Higgs and gauge boson couplings. The later are constrained by measurements of gauge boson pair production in  $e^+e^- \rightarrow W^+W^-$  at LEP2

and LC as well as  $W^+W^-$ ,  $W\gamma$ ,  $WZ$  production at the hadron colliders, TEVATRON and LHC. The best limits should come from LC and read [7]

$$\left| \frac{f_B}{\Lambda^2} \right| \lesssim 0.86 \text{ TeV}^{-2} \quad \text{or} \quad |\bar{f}_B| \lesssim 0.0056 \quad \text{or} \quad |\alpha_{B\Phi}| \lesssim 0.0028 , \quad (35)$$

$$\left| \frac{f_W}{\Lambda^2} \right| \lesssim 0.3 \text{ TeV}^{-2} \quad \text{or} \quad |\bar{f}_W| \lesssim 0.002 \quad \text{or} \quad |\alpha_{W\Phi}| \lesssim 0.001 . \quad (36)$$

$\mathcal{O}_{B\Phi}$  affects the  $HZZ$  and  $HZ\gamma$  couplings, while  $\mathcal{O}_{W\Phi}$  affects the  $HWW$ ,  $HZZ$  and  $HZ\gamma$  ones.

#### 4.1.4 $\mathcal{O}_{WW}$ and $\mathcal{O}_{BB}$

These "superblind" operators do not lead to anomalous gauge boson self couplings, but they affect the Higgs boson ones. Leaving aside rather loose constraints coming from loops involving Higgs, useful constraints will only come from Higgs boson production processes like  $q\bar{q}' \rightarrow HW$ ,  $e^+e^- \rightarrow HZ$ . For example at a LC one expects to reach, [4]

$$\left| \frac{f_{WW}}{\Lambda^2} \right| \lesssim 0.77 \text{ TeV}^{-2} \quad \text{or} \quad |d_W| \lesssim 0.005 , \quad (37)$$

$$\left| \frac{f_{BB}}{\Lambda^2} \right| \lesssim 1.1 \text{ TeV}^{-2} \quad \text{or} \quad |d_B| \lesssim 0.0025 . \quad (38)$$

These constraints can be further improved through the process  $\gamma\gamma \rightarrow H$  which should give [8]

$$\left| \frac{f_{WW}}{\Lambda^2} \right| \lesssim 0.15 \text{ TeV}^{-2} \quad \text{or} \quad |d_W| \lesssim 0.001 , \quad (39)$$

$$\left| \frac{f_{BB}}{\Lambda^2} \right| \lesssim 0.14 \text{ TeV}^{-2} \quad \text{or} \quad |d_B| \lesssim 0.0003 \quad (40)$$

$\mathcal{O}_{BB}$  induces  $HZZ$ ,  $HZ\gamma$  and  $H\gamma\gamma$  couplings, while  $\mathcal{O}_{WW}$  induces  $HWW$ ,  $HZZ$ ,  $HZ\gamma$  and  $H\gamma\gamma$  ones.

#### 4.1.5 $\mathcal{O}_{\Phi 2}$

The only effect of this "superblind" operator is to produce a wave function renormalization of the Higgs field, which modifies in a multiplicative way all Higgs boson couplings; (compare (A.3)). Its coupling constant will be first constrained by the  $e^+e^- \rightarrow HZ$  process. At LC it is expected to give [4]

$$\left| \frac{f_{\Phi,2}}{\Lambda^2} \right| \lesssim 0.53 \text{ TeV}^{-2} \quad \text{or} \quad |\bar{f}_{\Phi,2}| \lesssim 0.004 . \quad (41)$$

#### 4.1.6 $\mathcal{O}_{GG}$

This operator is the gluonic analogue of the electroweak  $\mathcal{O}_{WW}$  and  $\mathcal{O}_{BB}$  ones. It directly affects the  $Hgg$ ,  $Hggg$  couplings. It will be constrained by the rate and the  $p_T$  shape of Higgs production at hadron colliders through the process  $gg \rightarrow H$  and  $gg \rightarrow Hg$ . A recent analysis give the expected bound at LHC as [3]

$$|d_G| \lesssim 1.5 \times 10^{-4} . \quad (42)$$

This gluonic operator only concerns the  $Hgg$  and  $Hggg$  modes.

## 4.2 CP-violating operators

### 4.2.1 $\tilde{\mathcal{O}}_{BW}$

This is the CP-violating counterpart of  $\mathcal{O}_{BW}$ . It affects directly the  $HZZ$ ,  $HZ\gamma$  and  $H\gamma\gamma$  couplings.

Using the  $e^+e^- \rightarrow HZ$  process [4], one should get the constraint

$$|\frac{\tilde{f}_{BW}}{\Lambda^2}| \lesssim 0.7 \text{ TeV}^{-2} \quad \text{or} \quad |\tilde{f}_{BW}| \lesssim 0.017 , \quad (43)$$

while from the  $\gamma\gamma \rightarrow H$  process and generalizing the analysis in [8], one gets the estimate

$$|\frac{\tilde{f}_{BW}}{\Lambda^2}| \lesssim 0.22 \text{ TeV}^{-2} \quad \text{or} \quad |\tilde{f}_{BW}| \lesssim 0.005 . \quad (44)$$

### 4.2.2 $\tilde{\mathcal{O}}_{WW}$ and $\tilde{\mathcal{O}}_{BB}$

These are the CP-violating counterparts of  $\mathcal{O}_{WW}$  and  $\mathcal{O}_{BB}$ .  $\tilde{\mathcal{O}}_{BB}$  affects the  $HZZ$ ,  $HZ\gamma$  and  $H\gamma\gamma$  couplings; while  $\tilde{\mathcal{O}}_{WW}$  the  $HWW$ ,  $HZZ$ ,  $HZ\gamma$  and  $H\gamma\gamma$  ones.

Using the  $e^+e^- \rightarrow HZ$  process [4], one should get the constraint

$$|\frac{\tilde{f}_{WW}}{\Lambda^2}| \lesssim 0.77 \text{ TeV}^{-2} \quad \text{or} \quad |\tilde{d}_W| \lesssim 0.005 , \quad (45)$$

$$|\frac{\tilde{f}_{BB}}{\Lambda^2}| \lesssim 1.1 \text{ TeV}^{-2} \quad \text{or} \quad |\tilde{d}_B| \lesssim 0.0025 , \quad (46)$$

while from  $\gamma\gamma \rightarrow H$ , [8], one should get

$$|\frac{\tilde{f}_{WW}}{\Lambda^2}| \lesssim 0.5 \text{ TeV}^{-2} \quad \text{or} \quad |\tilde{d}_W| \lesssim 0.004 , \quad (47)$$

$$|\frac{\tilde{f}_{BB}}{\Lambda^2}| \lesssim 0.65 \text{ TeV}^{-2} \quad \text{or} \quad |\tilde{d}_B| \lesssim 0.0013 . \quad (48)$$

### 4.2.3 $\tilde{\mathcal{O}}_{GG}$

This is the CP-violating counterpart of  $\mathcal{O}_{GG}$ . It affects directly the  $Hgg$  and  $Hggg$  couplings. At LHC it is expected to give the constraint [3]

$$|\tilde{d}_G| \lesssim 7 \times 10^{-4} . \quad (49)$$

## 4.3 Fermionic operators, $\mathcal{O}_{f1}$

These operators induce purely Higgs-fermion anomalous interactions. No precise constraint are yet set on the strength of these couplings. The first one will come from the first study of the Higgs branching ratios at LC as discussed in Section 2.

We will express the coupling strength of these operators using (30), imposing  $f_{f1} = 4\pi$  and defining consequently the New Physics scale  $\Lambda_{NP}$  through:

$$g_{eff}^{f1} = \frac{4\pi}{\Lambda_{NP}^2} , \quad (50)$$

This scale can then be compared with other fermionic scales, for example those obtained from four-fermion contact interactions.

## 5 Step 2: Tests with branching ratios.

We now compare the experimental accuracies achievable in the Step 2 measurements of the Higgs branching ratios, (described in Section 2.2), to the corresponding relative shifts  $\delta^{NP,i}(F)$  on the various partial widths, defined in (31). The later are determined, for each of the NP operators, by the constraints given in Section 4. This comparison determines the sensitivity limits on NP, of each of the branching ratio measurements. The NP induced relative shift of partial width  $\delta^{NP,i}(F)$ , is connected to the corresponding one for the branching ratio by

$$\delta_B^{NP,i}(F) = \delta^{NP,i}(F) - \Sigma_F[B(F)\delta^{NP,i}(F)] . \quad (51)$$

Comparing it to the relative accuracy of the same branching ratio defined in (7) and demanding that

$$\delta_B(F) < \delta_B^{NP,i}(F) \quad (52)$$

for each operator and each channel, gives the minimum value of  $\bar{L}(\mu\mu)$  which is required for observing (through a muon Collider) possible NP effects which satisfy the constraints (possibly) imposed by the previously committed LHC and LC colliders.

These minimally required  $\bar{L}(\mu\mu)$  values are given in Fig.6a-m for each operator separately, using the most sensitive channels in each case. It must be noticed that the NP effect on a given branching ratio,  $\delta_B^{NP,i}(F)$ , may come either directly from the first term  $\delta^{NP,i}(F)$  in the channel considered, (compare (51)), or indirectly from the NP effect in another channel contributing to the sum  $\Sigma_F[B(F)\delta^{NP,i}(F)]$ . Below we always refer to such effects as *direct* and *indirect* respectively, and illustrate the results using  $m_H = 130 \text{ GeV}$ .

## 5.1 CP-conserving bosonic operators

$\mathcal{O}_{\Phi 1}$

See Fig.6a. Only the direct effect on the  $ZZ^*$  channel is accessible through the study of the branching ratios. As an example we note that for  $m_H = 130 \text{ GeV}$  this implies  $\bar{L}(\mu\mu) \gtrsim 413 \text{ fb}^{-1}$ .

This large value is due to two reasons. The first one is that this operator contributes to the very strongly constrained  $\Delta\rho$  quantity, while the second one arises from the rather weak accuracy with which the  $ZZ^*$  branching ratio can be measured.

$\mathcal{O}_{BW}$

See Fig.6b. The highest sensitivity comes directly from the SM depressed channel  $\gamma\gamma$ . For  $m_H = 130 \text{ GeV}$ , we get that  $\bar{L}(\mu\mu) \gtrsim 12(27) \text{ fb}^{-1}$  is needed in order to improve the constraints expected from LC (LC in  $\gamma\gamma$  mode).

$\mathcal{O}_{B\Phi}$

See Fig.6c. This operator does not affect the  $\gamma\gamma$  channel. The highest sensitivity appears directly from the  $Z\gamma$  and indirectly in the  $b\bar{b}$  channel. For  $m_H = 130 \text{ GeV}$ , we get from Fig.6c,  $\bar{L}(\mu\mu) \gtrsim 164 \text{ fb}^{-1}$  from the  $Z\gamma$ , while the *indirect*  $b\bar{b}$  and  $WW^*$  channels would require  $\bar{L}(\mu\mu) \gtrsim 483 \text{ fb}^{-1}$  and  $608 \text{ fb}^{-1}$ .

The results in Fig. 6c are based on the pessimistic attitude that  $\epsilon_{Z\gamma} \simeq 0.06$ , as suggested by the leptonic mode of the  $Z$  decay alone. Because of this, a high value of the luminosity is required. For an indication we note that if no reduction were applied ( $\epsilon_{Z\gamma} = 1$ ), the required luminosity would be  $11 \text{ fb}^{-1}$ .

$\mathcal{O}_{W\Phi}$

See Fig.6d. This operator does also not affect the  $\gamma\gamma$  channel, and the highest sensitivity comes directly from the  $WW^*$  one. For  $m_H = 130 \text{ GeV}$ , we get from  $WW^*$   $\bar{L}(\mu\mu) \gtrsim 53 \text{ fb}^{-1}$ ; whereas the *indirect*  $b\bar{b}$  channel requires  $\bar{L}(\mu\mu) \gtrsim 470 \text{ fb}^{-1}$ .

$\mathcal{O}_{WW}$

See Fig.6e. The highest sensitivity comes directly from the SM depressed channel  $\gamma\gamma$ . From this channel and using  $m_H = 130 \text{ GeV}$ , we conclude that  $\bar{L}(\mu\mu) > 0.7(27) \text{ fb}^{-1}$  is needed in order that the muon collider can improve the constraints from  $LC(LC_{\gamma\gamma})$ . The channels  $b\bar{b}$  (indirectly),  $WW^*$  (directly) and  $Z\gamma$  (directly), require respectively  $\bar{L}(\mu\mu) > 18(937) \text{ fb}^{-1}$ ,  $33(504) \text{ fb}^{-1}$  and  $34(510) \text{ fb}^{-1}$ .

$\mathcal{O}_{BB}$

See Fig.6f. The highest sensitivity comes from the SM depressed *direct* channel  $\gamma\gamma$ . For  $m_H = 130 \text{ GeV}$ , this requires  $\bar{L}(\mu\mu) \gtrsim 0.3(32) \text{ fb}^{-1}$ , for the muon collider to be able to improve the constraints from  $LC(LC_{\gamma\gamma})$ . The corresponding requirements for the *indirect*  $b\bar{b}$  and  $WW^*$  channels, are  $\bar{L}(\mu\mu) \gtrsim 8(789)$  and  $10(995) \text{ fb}^{-1}$ .

$\mathcal{O}_{\Phi 2}$

No constraint can be obtained on this operator from branching ratios alone.

$\tilde{\mathcal{O}}_{GG}$

See Fig.6g. The best constraint comes directly from the channel  $gg$ , which for  $m_H = 130 \text{ GeV}$  requires  $\bar{L}(\mu\mu) \gtrsim 0.8 \text{ fb}^{-1}$ . Indirectly, from the channels  $b\bar{b}$  and  $WW^*$ , one would need  $\bar{L}(\mu\mu) \gtrsim 7 \text{ fb}^{-1}$  and  $9 \text{ fb}^{-1}$ .

## 5.2 CP-violating operators

These operators affect the partial widths only quadratically in the coupling constants, since there is no interference with the SM amplitude, (see the Appendix). As a result the sensitivity tends to be weaker than for the CP-conserving operators. Nevertheless, the existing or near future constraints are so loose, that interesting improvements from a  $\mu^+\mu^-$  collider can be expected.

$\tilde{\mathcal{O}}_{BW}$

See Fig.6h. The highest sensitivity comes from the SM depressed *direct* channel  $\gamma\gamma$ . For  $m_H = 130 \text{ GeV}$ , by comparing to  $LC(LC_{\gamma\gamma})$  expectations, we require  $\bar{L}(\mu\mu) \gtrsim 0.2(21) \text{ fb}^{-1}$ . For the *indirect*  $b\bar{b}$  and  $WW^*$  channels, the corresponding requirement would be  $\bar{L}(\mu\mu) \gtrsim 5(675) \text{ fb}^{-1}$  and  $6(862) \text{ fb}^{-1}$ .

$\tilde{\mathcal{O}}_{WW}$

See Fig.6i. The highest sensitivity comes again directly from the SM depressed channel  $\gamma\gamma$ . For  $m_H = 130 \text{ GeV}$ , we get  $\bar{L}(\mu\mu) \gtrsim 15(36) \text{ fb}^{-1}$  from the  $\gamma\gamma$  channel, when comparing to the  $LC(LC_{\gamma\gamma})$  expectations. For the indirect  $b\bar{b}$  channel, and for the direct  $WW^*$  and  $Z\gamma$  ones, one would need  $\bar{L}(\mu\mu) > 162(396) \text{ fb}^{-1}$ ,  $207(506) \text{ fb}^{-1}$  and  $205(500) \text{ fb}^{-1}$  respectively.

$\tilde{\mathcal{O}}_{BB}$

See Fig.6j. The highest sensitivity comes again directly from the SM depressed channel  $\gamma\gamma$ . For  $m_H = 130 \text{ GeV}$ , this leads to  $\bar{L}(\mu\mu) \gtrsim 2(26) \text{ fb}^{-1}$ . Indirectly, from the  $b\bar{b}$  and  $WW^*$  channels, we would get  $\bar{L}(\mu\mu) \gtrsim 64(881) \text{ fb}^{-1}$  and  $81(1111) \text{ fb}^{-1}$ .

$\tilde{\mathcal{O}}_{GG}$

See Fig.6k. The best direct constraint comes from  $gg$ , which gives  $\bar{L}(\mu\mu) \gtrsim 3 \text{ fb}^{-1}$  for  $m_H = 130 \text{ GeV}$ . Indirectly, from the  $b\bar{b}$  and  $WW^*$  channels,  $\bar{L}(\mu\mu) > 30 \text{ fb}^{-1}$  and  $35 \text{ fb}^{-1}$  would be required.

## 5.3 Fermionic operators

$\mathcal{O}_{b1}$

See Fig.6l. As no constraint exists at present, we show for various values of  $m_H$ , the

luminosity as a function of  $\Lambda_{NP}$  defined in (50).

For  $m_H = 130 \text{ GeV}$  and using directly the  $b\bar{b}$  channel or indirectly the  $WW^*$  one, we conclude that a luminosity of  $1 \text{ fb}^{-1}$  ( $10 \text{ fb}^{-1}$ ) allows us to reach a scale  $\Lambda_{NP}$  of  $60 \text{ TeV}$  ( $105 \text{ TeV}$ ).

$$\mathcal{O}_{\mu 1}$$

See Fig.6m. We follow the same procedure as for  $\mathcal{O}_{b1}$ . The sensitivity is much higher because the SM coupling is reduced by the small value of the muon mass.

For  $m_H = 130 \text{ GeV}$  and using the total rate, a luminosity of  $1 \text{ fb}^{-1}$  ( $10 \text{ fb}^{-1}$ ) allows to reach a scale  $\Lambda_{NP}$  of  $500 \text{ TeV}$  ( $900 \text{ TeV}$ ).

Summarizing this Step 2, for a light Higgs ( $m_H \lesssim 160 \text{ GeV}$ ), one would expect that the study of the Higgs branching ratios at a  $\mu^+\mu^-$  collider should supply improvements for many NP operators (except  $\mathcal{O}_{\Phi,1}$ ,  $\mathcal{O}_{\Phi,2}$ ,  $\mathcal{O}_{B\Phi}$ ) provided that a luminosity of a few  $\text{fb}^{-1}$  could be accumulated. This should be true, even if the  $\gamma\gamma$  collisions are realized at LC before the muon collider. For higher Higgs masses, the Higgs total width increases, so that the peak cross section decreases, and together with it the number of events and the accuracy. In addition the branching ratios of the preferred modes for NP tests, like  $\gamma\gamma$ ,  $Z\gamma$ ,  $gg$  (and  $b\bar{b}$ ), also decrease. On the opposite the  $WW$  and  $ZZ$  branching ratios increase but the sensitivity to NP in these channel is weaker, since they are not enhanced by the loop factor  $(\alpha/\pi)^{-1}$ , like in the previous modes. In addition the real  $WW$  background increases. So in the whole, the possibility of NP tests is quickly depressed. This can be seen in Fig.6a-m. Even with  $\bar{L}(\mu\mu)$  of the order of  $100 \text{ fb}^{-1}$ , the improvements with respect to LC and LHC stop for all operators around  $m_H \simeq 160 \text{ GeV}$ .

## 6 Step 3: Tests with total and partial widths

We now directly compare the experimental relative accuracy on the total width  $\bar{\delta}_\Gamma$  (compare (12)), obtained from the line shape, to the relative NP effect on the total width  $\Sigma_F B(F) \delta^{NP,i}(F)$  appearing in (51). In addition, we also compare the individual relative accuracies on the partial widths  $\delta_\Gamma(F)$  (compare (13)), to the corresponding NP quantities  $\delta^{NP,i}(F)$  defined in (31).

For the NP operators discussed in Section 4, we expect

- From the total width: An improvement for the operators contributing to the main Higgs decay modes ( $b\bar{b}$ ,  $WW$ ,  $ZZ$ ), especially those which are not much constrained by the study of the branching ratios. This is the case for  $\mathcal{O}_{\Phi,1}$ ,  $\mathcal{O}_{\Phi,2}$ ,  $\mathcal{O}_{B\Phi}$  and  $\mathcal{O}_{b1}$ .
- From the partial widths: An improvement on operators whose effects are hidden when considering branching ratios. This is especially the case of  $\mathcal{O}_{\Phi,2}$ , but partially also for  $\mathcal{O}_{\Phi,1}$ .

The results for  $\mathcal{O}_{\Phi,1}$  and  $\mathcal{O}_{\Phi,2}$  are shown in Figs.7a,b, while in Figs.8a-d for  $\mathcal{O}_{b1}$ . The main gain is for  $\mathcal{O}_{\Phi 2}$  which was not at all constrained from the study of the branching

ratios. For  $m_H = 130 \text{ GeV}$ , a reasonable accuracy  $\bar{\delta}_\Gamma = 0.03/\sqrt{\bar{L}(\mu\mu)}$ , (implied by an error of  $0.15 \text{ MeV}$  on the total width for  $\bar{L}_{\mu\mu} = 1 \text{ fb}^{-1}$ ), allows to improve the constraint on  $\mathcal{O}_{\Phi 2}$ , as soon as  $\bar{L}(\mu\mu) \gtrsim 1 \text{ fb}^{-1}$ . In fact, for this operator, the measurement of the total width is equally good (for low  $m_H$ ) or better (for higher  $m_H$ ), than any other partial width measurement, including  $b\bar{b}$ .

For  $\mathcal{O}_{\Phi 1}$ , the  $400 \text{ fb}^{-1}$  luminosity level required by the study of the branching ratios, could be reduced in the case of a light Higgs boson if  $\bar{\delta}_\Gamma \lesssim 0.02/\sqrt{\bar{L}(\mu\mu)}$ . Thus, for  $m_H = 130 \text{ GeV}$  and  $\bar{L}(\mu\mu) \simeq 100 \text{ fb}^{-1}$ , this means an accuracy of about  $0.01 \text{ MeV}$  on the total width, which is probably difficult to achieve.

For  $\mathcal{O}_{b1}$ , as well as for  $\mathcal{O}_{B\Phi}$ , the results obtained from the study of the branching ratios, could be improved if an accuracy of about  $\bar{\delta}_\Gamma \lesssim 0.01/\sqrt{\bar{L}_{\mu\mu}}$  is attained. For other operators, like *e.g.* the CP-violating ones, the required  $\bar{\delta}_\Gamma$  is even smaller, and is surely unachievable.

## 7 Conclusions

We have found that a  $\mu^+\mu^-$  collider working as a Higgs factory, can improve the knowledge of the couplings of a light Higgs boson, as soon as a luminosity of the order of a few  $\text{fb}^{-1}$  is accumulated. This applies to Higgs bosons whose mass is below the  $WW$  threshold ( $m_H \lesssim 2M_W$ ), so that  $\Gamma_H$  is small enough to give the peak cross section as an enhancement.

This strategy is no more valid for  $m_H \gtrsim 2M_W$ , since the Higgs width becomes too broad, and the associated increasing dominance of the  $WW$  and  $ZZ$  channels (which are less sensitive to NP), makes the use of the extremely rare  $\gamma\gamma$ ,  $Z\gamma$  and  $gg$  channels less efficient.

In the present work, we have first checked that with a luminosity of a fraction of  $\text{fb}^{-1}$ , the measurement of the Higgs branching ratios at the  $\mu^+\mu^-$  collider should improve the one done at LC through  $e^+e^- \rightarrow HZ$ .

To be more quantitative about the meaning of testing the Higgs boson couplings, we have subsequently considered a set of  $\text{dim} = 6$   $SU(3) \times SU(2) \times U(1)$  gauge invariant operators, consisting of the 8 bosonic CP-conserving ones called  $\mathcal{O}_{\Phi 1}$ ,  $\mathcal{O}_{BW}$ ,  $\mathcal{O}_{B\Phi}$ ,  $\mathcal{O}_{W\Phi}$ ,  $\mathcal{O}_{WW}$ ,  $\mathcal{O}_{BB}$ ,  $\mathcal{O}_{\Phi 2}$ ,  $\mathcal{O}_{GG}$ ; the 4 bosonic CP-violating ones  $\tilde{\mathcal{O}}_{BW}$ ,  $\tilde{\mathcal{O}}_{WW}$ ,  $\tilde{\mathcal{O}}_{BB}$ ,  $\tilde{\mathcal{O}}_{GG}$ ; and the fermionic operators  $\mathcal{O}_{f1}$ .

For each of them, we have established the minimal  $\bar{L}(\mu\mu)$  luminosity needed in order to improve the constraints expected from the colliders LEP, SLC and LC (in  $e^+e^-$  and  $\gamma\gamma$  modes), as well as the hadronic colliders TEVATRON and LHC; all of which should run earlier.

One indeed finds that for most of the operators (except for  $\mathcal{O}_{\Phi,1}$ ,  $\mathcal{O}_{\Phi,2}$ ,  $\mathcal{O}_{B\Phi}$ ) a few  $\text{fb}^{-1}$  will be sufficient as long as  $m_H \lesssim 2M_W$ ; see Fig.9a,b. In the case of  $\mathcal{O}_{BW}$ ,  $\mathcal{O}_{WW}$ ,  $\mathcal{O}_{BB}$  and their CP-violating partners, the results depend on whether the  $\gamma\gamma$  mode at LC will run before the  $\mu^+\mu^-$  collider. If this indeed happens, then for the muon Collider to do better, luminosities in the range  $10 - 20 \text{ fb}^{-1}$  are required. Otherwise a fraction of  $\text{fb}^{-1}$  should be sufficient. An additional measurement of the total width  $\Gamma_H$  at the level

of ten percent will allow to improve the constraints on  $\mathcal{O}_{\Phi,2}$ . But in order to improve  $\mathcal{O}_{\Phi,1}$ ,  $\mathcal{O}_{b1}$  and  $\mathcal{O}_{B\Phi}$  also, an accuracy at percent level is required.

In Tables 3,4, we illustrate the results for the case of  $m_H = 130 \text{ GeV}$ . The numbers in parenthesis refer to the comparison with the  $\gamma\gamma$  mode at LC.

**Table 3: Required  $\mu^+\mu^-$  luminosity in  $fb^{-1}$  for  $m_H = 130 \text{ GeV}$   
CP-conserving operators**

$\mathcal{O}_{\Phi 1}$	$\mathcal{O}_{BW}$	$\mathcal{O}_{B\Phi}$	$\mathcal{O}_{W\Phi}$	$\mathcal{O}_{WW}$	$\mathcal{O}_{BB}$	$\mathcal{O}_{\Phi 2}$	$\mathcal{O}_{GG}$
413	12(27)	164	53	0.7(27)	0.3(32)	1.	0.8

**Table 4: Required  $\mu^+\mu^-$  luminosity in  $fb^{-1}$  for  $m_H = 130 \text{ GeV}$   
CP-violating and fermionic operators**

$\mathcal{O}_{BW}$	$\mathcal{O}_{WW}$	$\mathcal{O}_{BB}$	$\mathcal{O}_{GG}$	$\mathcal{O}_{b1}(\Lambda = 50 \text{ TeV})$	$\mathcal{O}_{\mu 1}(\Lambda = 500 \text{ TeV})$
0.2(21)	15(36)	2(26)	3	0.7	1

Concerning the comparison of  $\mu C$  and LC, we should remember that the above results are based on the assumption that  $\bar{L}(ee) \simeq 100 fb^{-1}$ . They should be appropriately scaled up, if (as is currently contemplated), a higher average integrated luminosity  $\bar{L}(ee)$  is achieved which may even reach the level of  $500 fb^{-1}$ .

In the case of CP-violating operators, we have based our study only on the quadratic effects in the partial widths. We have left the detailed study of CP-violating asymmetries for a separate work.

Concerning the fermionic operators, as there will be no other previous constraints than those coming from branching ratios measured at LC, improvements will come as soon as the statistics becomes better than at LC; compare Fig.5 and Tables 2a,b. Thus, for  $m_H = 130 \text{ GeV}$ , a luminosity of a fraction of  $fb^{-1}$  is sufficient. We also note that a luminosity of  $1 fb^{-1}$  will allow to test fermionic scales of the order of 60, 500 TeV for  $\mathcal{O}_{b1}$ ,  $\mathcal{O}_{\mu 1}$  respectively. Such scales are much higher than those accessible at HERA, LHC and LC for four-fermion operators. It should be remarked though, that the present Higgs-fermion operators are of totally different nature and are perhaps more closely connected to the role of NP in the mass generation mechanism.

We also notice that the values of the NP scales to which these new constraints will correspond, (through unitarity relations [13, 9]), lie in the range of several tens of TeV. This is a domain where many theoretical models expect NP to show up. If anomalous events were observed at such a Higgs factory, the disentangling of the possibly contributing operators would be the next important task. From the channels in which these anomalous effects would appear, it should be possible to identify a restricted set of operators. This would be useful for determining the structure of NP; i.e. the role of flavour, of colour and of spin.

### Acknowledgments

We like to thank A. Blondel and P. Janot for useful informations about the muon collider project and several experimental considerations.

## Appendix A: The partial decay widths of the Higgs boson

In this appendix we define the partial widths for the decay  $H \rightarrow F$  of an off-shell Higgs particle by

$$\Gamma_{H \rightarrow F}(s) = \frac{(2\pi)^4}{2m_H} \int |T_{H \rightarrow F}(s)|^2 d\Phi_F , \quad (\text{A.1})$$

where  $\Phi_F$  gives the usual definition of the invariant phase space [14]. Note that the off-shellness only appears in the invariant amplitude  $T_{H \rightarrow F}(s)$ .

### A.1 $H \rightarrow \gamma\gamma$ .

Contributions to this process arise from the SM at 1 loop [15], and from operators  $\mathcal{O}_{BW}$ ,  $\mathcal{O}_{WW}$ ,  $\mathcal{O}_{BB}$ , their CP-violating partners, and also  $\mathcal{O}_{\Phi,1}$ ,  $\mathcal{O}_{\Phi,2}$  from  $Z_H$ . The result is

$$\begin{aligned} \Gamma_{H \rightarrow \gamma\gamma}(s) = & \frac{\sqrt{2}G_F}{16\pi m_H} s^2 \left\{ \left| \frac{\alpha}{4\pi} \left( \frac{4}{3}F_t + F_W \right) \sqrt{Z_H} - 2d_W s_W^2 - 2d_B c_W^2 + \bar{f}_{BW} s_W c_W \right|^2 \right. \\ & \left. + \left| 2\tilde{d}_W s_W^2 + 2\tilde{d}_B c_W^2 - \tilde{f}_{BW} s_W c_W \right|^2 \right\} , \end{aligned} \quad (\text{A.2})$$

in which the Higgs wave function renormalization  $Z_H$  is determined by the tree level NP contribution of  $\mathcal{O}_{\Phi,1}$ ,  $\mathcal{O}_{\Phi,2}$  and is given by

$$Z_H = [1 + 8\bar{f}_{\Phi,2} + \frac{1}{2}\bar{f}_{\Phi,1}]^{-1} , \quad (\text{A.3})$$

while the standard contribution arises from top and  $W$  loops respectively determined by

$$F_t = -2t_t(1 + (1 - t_t)f(t_t)) , \quad (\text{A.4})$$

$$F_W = 2 + 3t_W + 3t_W(2 - t_W)f(t_W) , \quad (\text{A.5})$$

in terms of

$$\begin{aligned} f(t) &= \left[ \sin^{-1}(1/\sqrt{t}) \right]^2 & \text{if} & \quad t \geq 1 , \\ f(t) &= -\frac{1}{4} \left[ \ln \left( \frac{1 + \sqrt{1-t}}{1 - \sqrt{1-t}} \right) - i\pi \right]^2 & \text{if} & \quad t < 1 , \end{aligned} \quad (\text{A.6})$$

where  $t_t = 4m_t^2/s$  and  $t_W = 4m_W^2/s$ .

### A.2 $H \rightarrow \gamma Z$ .

Contributions arise here also from the SM 1 loop top and  $W$  contributions [15], as well as from  $\mathcal{O}_{BW}$ ,  $\mathcal{O}_{WW}$ ,  $\mathcal{O}_{BB}$ , their CP violating analogs, and also from the operators  $\mathcal{O}_{B\Phi}$

,  $\mathcal{O}_{W\Phi}$ ,  $\mathcal{O}_{\Phi,1}$ ,  $\mathcal{O}_{\Phi,2}$ . The result is

$$\begin{aligned}\Gamma_{H \rightarrow \gamma Z}(s) = & \frac{\sqrt{2}G_F s^2}{8\pi m_H} \left(1 - \frac{M_Z^2}{s}\right)^3 \left( \left| \frac{\alpha}{4\pi} (A_t + A_W) \sqrt{Z_H} + 2(d_W - d_B) s_W c_W \right. \right. \\ & - \frac{1}{2} (c_W^2 - s_W^2) \bar{f}_{BW} - \frac{s_W}{2c_W} (\bar{f}_B - \bar{f}_W) \left. \right|^2 \\ & \left. + \left| 2(\tilde{d}_W - \tilde{d}_B) s_W c_W - \frac{1}{2} (c_W^2 - s_W^2) \tilde{f}_{BW} \right|^2 \right),\end{aligned}\quad (\text{A.7})$$

with

$$A_t = \frac{(-6 + 16s_W^2)}{3s_W c_W} [I_1(t_t, l_t) - I_2(t_t, l_t)] \quad , \quad (\text{A.8})$$

$$A_W = -\cot \theta_W [4(3 - \tan^2 \theta_W) I_2(t_W, l_W) + [(1 + \frac{2}{t_W}) \tan^2 \theta_W - (5 + \frac{2}{t_W})] I_1(t_W, l_W)] \quad , \quad (\text{A.9})$$

where  $t_t = 4m_t^2/s$ ,  $t_W = 4M_W^2/s$  as before, and  $l_t = 4m_t^2/M_Z^2$ ,  $l_W = 4M_W^2/M_Z^2$ , and

$$I_1(a, b) = \frac{ab}{2(a-b)} + \frac{a^2b^2}{2(a-b)^2} [f(a) - f(b)] + \frac{a^2b}{(a-b)^2} [g(a) - g(b)] \quad , \quad (\text{A.10})$$

$$I_2(a, b) = -\frac{ab}{2(a-b)} [f(a) - f(b)] \quad , \quad (\text{A.11})$$

$f(t)$  is given in (A.6) and

$$\begin{aligned}g(t) &= \sqrt{t-1} \sin^{-1} \left( \frac{1}{\sqrt{t}} \right) \quad \text{if} \quad t \geq 1 \quad , \\ g(t) &= \frac{1}{2} \sqrt{1-t} \left[ \ln \left( \frac{1 + \sqrt{1-t}}{1 - \sqrt{1-t}} \right) - i\pi \right] \quad \text{if} \quad t < 1 \quad .\end{aligned}\quad (\text{A.12})$$

### A.3 $H \rightarrow gg$ .

Contributions arise from the SM 1-loop top exchanges and from tree level contribution of the operators  $\mathcal{O}_{GG}$  and  $\mathcal{O}_{\Phi 1}$ ,  $\mathcal{O}_{\Phi 2}$ . The result is

$$\Gamma_{H \rightarrow gg}(s) = \frac{s^2}{8\pi m_H} \left[ 1 + \left( \frac{95}{4} - \frac{7N_F}{6} \right) \frac{\alpha_s}{\pi} \right] \left[ |A_{SM} \sqrt{Z_H} - \frac{4\tilde{d}_G}{v}|^2 + \left| \frac{4\tilde{d}_G}{v} \right|^2 \right] \quad , \quad (\text{A.13})$$

where

$$A_{SM} = -\frac{\alpha_s t_t}{2\pi v} (1 + (1 - t_t) f(t_t)) \quad , \quad (\text{A.14})$$

with  $t_t = 4m_t^2/s$  and  $f(t)$  given in (A.6). Note the presence of an important QCD correction factor which, (for the number of light quark flavours  $N_F = 5$ ) is of the order of 65%.

## A.4 $H \rightarrow WW$ .

Contributions arise from the SM at tree level and from operators  $\mathcal{O}_{W\Phi}$ ,  $\mathcal{O}_{WW}$ ,  $\tilde{\mathcal{O}}_{WW}$ , as well as from  $\mathcal{O}_{\Phi 1}$ ,  $\mathcal{O}_{\Phi 2}$  which induce a wave function renormalization of the Higgs field. For  $m_H > 2M_W$ , we get

$$\begin{aligned}\Gamma_{H \rightarrow W^+W^-}(s) &= \frac{\alpha\beta_W}{16s_W^2M_W^2m_H} \left( 2 \left[ 2M_W^2\sqrt{Z_H} - 2d_W(s - 2M_W^2) - \bar{f}_W s \right]^2 \right. \\ &\quad + \left[ \sqrt{Z_H}(s - 2M_W^2) - 4d_W M_W^2 - \bar{f}_W s \right]^2 \\ &\quad \left. + 8|\tilde{d}_W|^2 s(s - 4M_W^2) \right) \end{aligned}\quad (\text{A.15})$$

in which  $\beta_W = \sqrt{1 - 4M_W^2/s}$ .

For  $M_W < m_H < 2M_W$ , the Higgs decay width is computed with one virtual gauge boson decaying into a lepton or quark pair. The expression is [15, 16, 3]

$$\begin{aligned}\Gamma_{H \rightarrow WW^*}(s) &= \frac{3\alpha^2 s}{32\pi m_H s_W^4} \left[ \left( \sqrt{Z_H} - \frac{\bar{f}_W}{2x} \right)^2 D_{SM}(x) + d_W \sqrt{Z_H} D_1(x) - \bar{f}_W \sqrt{Z_H} D_4(x) \right. \\ &\quad \left. + 8d_W^2 D_2(x) + \bar{f}_W^2 D_5(x) - d_W \bar{f}_W D_6(x) + 8|\tilde{d}_W|^2 D_3(x) \right] \end{aligned}\quad (\text{A.16})$$

where  $x = m_W^2/s$  and

$$\begin{aligned}D_{SM}(x) &= \frac{3(20x^2 - 8x + 1)}{\sqrt{4x - 1}} \cos^{-1} \left( \frac{3x - 1}{2x^{3/2}} \right) \\ &\quad - (1 - x) \left( \frac{47x}{2} - \frac{13}{2} + \frac{1}{x} \right) - 3(2x^2 - 3x + \frac{1}{2}) \ln(x) \quad , \end{aligned}\quad (\text{A.17})$$

$$\begin{aligned}D_1(x) &= \frac{24(14x^2 - 8x + 1)}{\sqrt{4x - 1}} \cos^{-1} \left( \frac{3x - 1}{2x^{3/2}} \right) \\ &\quad + 12(x - 1)(9x - 5) - 12(2x^2 - 6x + 1) \ln(x) \quad , \end{aligned}\quad (\text{A.18})$$

$$\begin{aligned}D_2(x) &= \frac{54x^3 - 40x^2 + 11x - 1}{x\sqrt{4x - 1}} \cos^{-1} \left( \frac{3x - 1}{2x^{3/2}} \right) \\ &\quad + \frac{(x - 1)}{6} \left( 89x - 82 + \frac{17}{x} \right) - \left( 3x^2 - 15x + \frac{9}{2} - \frac{1}{2x} \right) \ln(x) \quad , \end{aligned}\quad (\text{A.19})$$

$$\begin{aligned}D_3(x) &= \frac{-28x^2 + 11x - 1}{x\sqrt{4x - 1}} \cos^{-1} \left( \frac{3x - 1}{2x^{3/2}} \right) \\ &\quad - \frac{x^2}{6} - \frac{21x}{2} + \frac{27}{2} - \frac{17}{6x} + \frac{(6x^2 - 9x + 1)}{2x} \ln(x) \quad , \end{aligned}\quad (\text{A.20})$$

$$\begin{aligned}
D_4(x) &= -\sqrt{4x-1} \frac{(10x-4)}{x} \cos^{-1} \left( \frac{3x-1}{2x^{3/2}} \right) \\
&\quad - \frac{(x-1)}{3x^2} (2x^3 + 50x^2 - 31x + 3) + (6x - 9 + \frac{2}{x}) \ln(x) \quad , \quad (\text{A.21})
\end{aligned}$$

$$\begin{aligned}
D_5(x) &= \frac{3\sqrt{4x-1}}{4x^2} \cos^{-1} \left( \frac{3x-1}{2x^{3/2}} \right) \\
&\quad + \frac{1}{16x^3} (1-x)(x^4 - 7x^3 - 9x^2 - 25x + 4) - \frac{3}{4x^2} (x^2 + x - \frac{1}{2}) \ln(x) \quad (\text{A.22})
\end{aligned}$$

$$\begin{aligned}
D_6(x) &= \frac{4(14x^2 - 13x + 2)}{x\sqrt{4x-1}} \cos^{-1} \left( \frac{3x-1}{2x^{3/2}} \right) + \frac{2(1-x)}{3x} (x^2 - 17x + 28) \\
&\quad + 2(9 - \frac{2}{x}) \ln(x) \quad . \quad (\text{A.23})
\end{aligned}$$

## A.5 $H \rightarrow ZZ$ .

Contributions arise from the SM at tree level and from operators  $\mathcal{O}_{BW}$ ,  $\mathcal{O}_{B\Phi}$ ,  $\mathcal{O}_{W\Phi}$ ,  $\mathcal{O}_{WW}$ ,  $\mathcal{O}_{BB}$ ,  $\tilde{\mathcal{O}}_{BW}$ ,  $\tilde{\mathcal{O}}_{WW}$ ,  $\tilde{\mathcal{O}}_{BB}$  as well as  $\mathcal{O}_{\Phi 1}$ ,  $\mathcal{O}_{\Phi 2}$  through the wave function renormalization of the Higgs field. For  $m_H > 2M_Z$ , we get

$$\begin{aligned}
\Gamma_{H \rightarrow ZZ}(s) &= \frac{\alpha\beta_Z}{32s_W^2 M_W^2 m_H} \left( 2 \left[ 2M_Z^2 (\sqrt{Z_H} + \bar{f}_{\Phi 1}) \right. \right. \\
&\quad \left. \left. - (2d_B s_W^2 + 2d_W c_W^2 + \bar{f}_{BW} s_W c_W)(s - 2M_Z^2) - (\bar{f}_W + \bar{f}_B \frac{s_W^2}{c_W^2})s \right]^2 \right. \\
&\quad \left. + \left[ (\sqrt{Z_H} + \bar{f}_{\Phi 1})(s - 2M_Z^2) - 2M_Z^2 (2d_B s_W^2 + 2d_W c_W^2 \right. \right. \\
&\quad \left. \left. + \bar{f}_{BW} s_W c_W) - (\bar{f}_W + \bar{f}_B \frac{s_W^2}{c_W^2})s \right]^2 \right. \\
&\quad \left. + 2 \left| (2\tilde{d}_B s_W^2 + 2\tilde{d}_W c_W^2 + \tilde{\bar{f}}_{BW} s_W c_W) \right|^2 M_H^2 (s - 4M_Z^2) \right) , \quad (\text{A.24})
\end{aligned}$$

with  $\sqrt{Z_H}$  given by eq.(A.3) and  $\beta_Z = \sqrt{1 - 4M_Z^2/s}$ .

For  $M_Z < m_H < 2M_Z$ , we get

$$\begin{aligned}
\Gamma_{H \rightarrow ZZ^*}(s) &= \frac{\alpha^2 s}{128\pi m_H s_W^4 c_W^4} \left( 7 - \frac{40s_W^2}{3} + \frac{160s_W^4}{9} \right) \cdot \\
&\quad \left[ \left( \sqrt{Z_H} + \bar{f}_{\Phi 1} - \frac{1}{2x} (\bar{f}_W + \bar{f}_B \frac{s_W^2}{c_W^2}) \right)^2 D_{SM}(x) \right. \\
&\quad \left. + (\sqrt{Z_H} + \bar{f}_{\Phi 1}) \left( d_B s_W^2 + d_W c_W^2 + \frac{\bar{f}_{BW}}{2} c_W s_W \right) D_1(x) \right]
\end{aligned}$$

$$\begin{aligned}
& -(\sqrt{Z_H} + \bar{f}_{\Phi,1}) \left( \bar{f}_W + \bar{f}_B \frac{s_W^2}{c_W^2} \right) D_4(x) \\
& + 2(2d_B s_W^2 + 2d_W c_W^2 + \bar{f}_{BW} s_W c_W)^2 D_2(x) + \left( \bar{f}_W + \bar{f}_B \frac{s_W^2}{c_W^2} \right)^2 D_5(x) \\
& + \frac{1}{2}(2d_B s_W^2 + 2d_W c_W^2 + \bar{f}_{BW} s_W c_W) \left( \bar{f}_W + \bar{f}_B \frac{s_W^2}{c_W^2} \right) D_6(x) \\
& + 2|(2\tilde{d}_B s_W^2 + 2\tilde{d}_W c_W^2 + \tilde{f}_{BW} s_W c_W)|^2 D_3(x) \Big] \tag{A.25}
\end{aligned}$$

where  $x = M_Z^2/s$ .

## A.6 $H \rightarrow f\bar{f}$ .

Contributions arise from the SM at tree level, from operators  $\mathcal{O}_{\Phi,1}$ ,  $\mathcal{O}_{\Phi,2}$  through the wave function renormalization of the Higgs field  $Z_H$ , (compare (A.3)), and from the fermionic operator  $\mathcal{O}_{f1}$ . We find

$$\Gamma_{H \rightarrow f\bar{f}}(s) = \frac{N_c s}{8\pi m_H} \beta_f^3 \left| -\frac{m_f}{v} \sqrt{Z_H} + \frac{3}{2\sqrt{2}} \bar{f}_{f1} \right|^2 \tag{A.26}$$

with the colour factor

$$N_c = 1 \quad \text{for leptons} , \tag{A.27}$$

$$N_c = 3(1 + 5.67 \frac{\alpha_s}{\pi}) \quad \text{for quarks} , \tag{A.28}$$

and  $\beta_f = \sqrt{1 - 4m_f^2/s}$ . In the case of quarks ( $f = q$ ), the mass  $m_f$  is the running mass  $m_q(m_H)$  computed with the expression given in ref.[2].

## References

- [1] J.F. Gunion, hep-ph/9703203; V. Barger, hep-ph/9803480; D.B. Cline, *Int. J. Mod. Phys. A***13** (1998) 183; and references therein.
- [2] M. Spira, hep-ph/9705337, *Fortsch. Phys.* **46** (1998) 203.
- [3] G.J. Gounaris, J. Layssac and F.M.Renard, hep-ph/9803422, *Phys. Rev. D***58** (1998) 075006.
- [4] K.Hagiwara and M.L. Stong, *Z. f. Phys. C***62** (1994) 99; G.J. Gounaris, F.M.Renard and N.D. Vlachos *Nucl. Phys. B***459** (1996) 51.
- [5] K.Hagiwara, S.Ishihara, R.Szalapski, D.Zeppenfeld, *Phys. Lett. B***283** (1992) 353 and *Phys. Rev. D***48** (1993) 2182
- [6] K. Hagiwara, S. Matsumoto, and R. Szalapski, *Phys. Lett. B***357** (1995) 411
- [7] G.J. Gounaris and C.G. Papadopoulos, *Eur. Phys. J. C***62** (1998) 365, hep-ph/9612378; G.J. Gounaris and C.G. Papadopoulos,  $e^+e^-$  Linear Colliders, Physics and Detector studies, Part E, DESY-97-123E(1997), ed. R. Settles, p.143; G. Daskalakis, *ibid*, p.157.
- [8] G.J. Gounaris and F.M.Renard, *Z. f. Phys. C***69** (1996) 513
- [9] G.J. Gounaris, D.T. Papadamou and F.M. Renard, *Z. f. Phys. C***76** (1997) 333, hep-ph/9609437.
- [10] G.J. Gounaris and G. Tsirigoti, *Phys. Rev. D***56** (1997) 3030.
- [11] M.Peskin and T.Takeuchi, *Phys. Rev. D***46** (1992) 381.
- [12] G. Altarelli, R. Barbieri and F. Caravaglios *Phys. Lett. B***314** (1993) 357
- [13] G.J.Gounaris, J.Layssac, J.E.Paschalis and F.M.Renard, *Z. f. Phys. C***66** (1995) 619; G.J. Gounaris, F.M. Renard and G. Tsirigoti, *Phys. Lett. B***350** (1995) 212.
- [14] Particle Data Group, *Eur. Phys. J. C***3** (1998) 1.
- [15] J.F. Gunion, H.E. Haber, G. Kane and S. Dawson, *The Higgs Hunter's Guide*, Adison-Wesley, Redwood City, Ca, 1990.
- [16] V. Barger, K. Cheung, A Djouadi, B.A. Kniehl and P.M. Zerwas, *Phys. Rev. D***49** (1994) 79; W.-Y. Keung and W.J. Marciano *Phys. Rev. D***30** (1984) 248.

## Figure captions

**Fig.1** Total SM Higgs width versus  $m_H$ .

**Fig.2** SM Higgs branching ratios versus  $m_H$ .

**Fig.3** Convolved peak  $\mu^+\mu^- \rightarrow H$  cross section versus  $m_H$ .

**Fig.4** Maximal  $e^+e^- \rightarrow HZ$  cross section versus  $m_H$ .

**Fig.5** Ratio  $\bar{L}(\mu\mu)/\bar{L}(ee)$  required to get the same number of events in  $\mu^+\mu^- \rightarrow H$  and in  $e^+e^- \rightarrow HZ$ , versus  $m_H$ .

**Fig.6**  $\mu^+\mu^-$  luminosity needed to improve the constraint on operator  $\mathcal{O}_{\Phi 1}$  (a),  $\mathcal{O}_{BW}$  (b),  $\mathcal{O}_{B\Phi}$  (c),  $\mathcal{O}_{W\Phi}$  (d),  $\mathcal{O}_{WW}$  (e),  $\mathcal{O}_{BB}$  (f),  $\mathcal{O}_{GG}$  (g);  $\tilde{\mathcal{O}}_{BW}$  (h),  $\tilde{\mathcal{O}}_{WW}$  (i),  $\tilde{\mathcal{O}}_{BB}$  (j),  $\tilde{\mathcal{O}}_{GG}$  (k);  $\mathcal{O}_{b1}$  (l),  $\mathcal{O}_{\mu 1}$  (m).

**Fig.7**  $\mu^+\mu^-$  luminosity needed to improve the constraint on operator  $\mathcal{O}_{\Phi 1}$  (a),  $\mathcal{O}_{\Phi 2}$  (b), when the total width is measured with a relative accuracy parameter  $\delta_\Gamma$  as indicated.

**Fig.8**  $\mu^+\mu^-$  luminosity needed to improve the constraint on operator  $\mathcal{O}_{b1}$  versus the fermionic scale  $\Lambda_{NP}$  for various values of  $m_H$  and for accuracies on the total width measurement,  $\delta_\Gamma = 0.005$  (a),  $\delta_\Gamma = 0.01$  (b),  $\delta_\Gamma = 0.03$  (c),  $\delta_\Gamma = 0.05$  (d).

**Fig.9**  $\mu^+\mu^-$  luminosity needed to improve the constraints on the CP-conserving operators (only the most efficient channel is indicated).

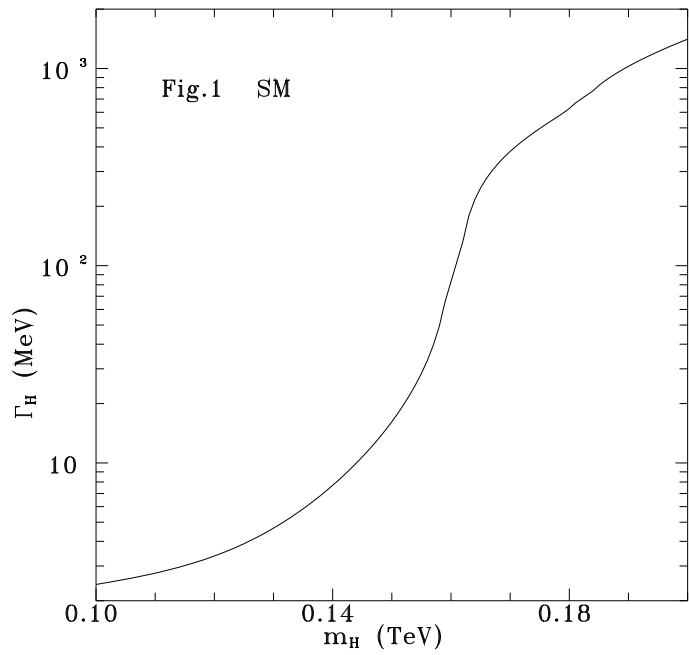


Figure 1: Total SM Higgs width versus  $m_H$ .

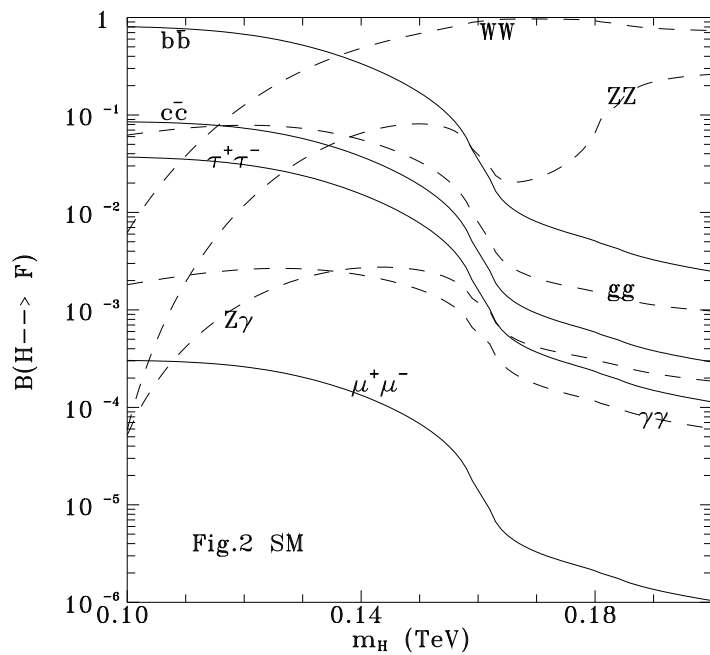


Figure 2: SM Higgs branching ratios versus  $m_H$ .

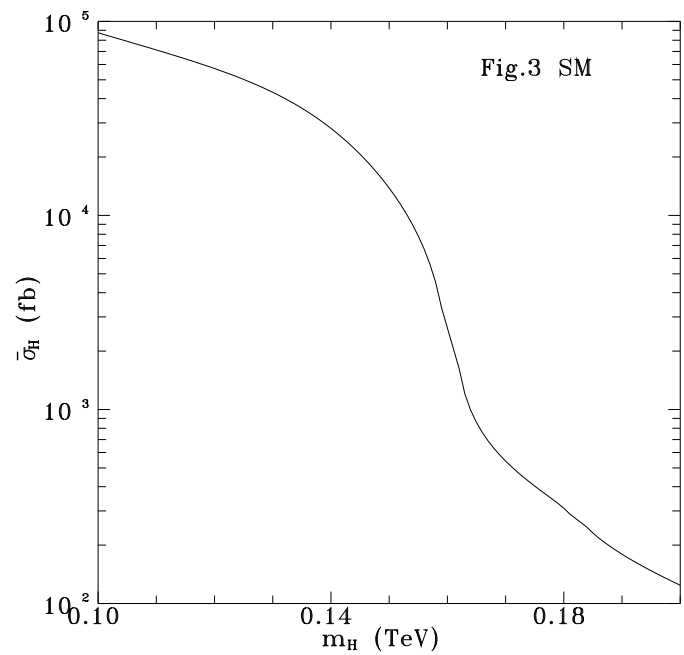


Figure 3: Convoluted peak  $\mu^+ \mu^- \rightarrow H$  cross section versus  $m_H$ .

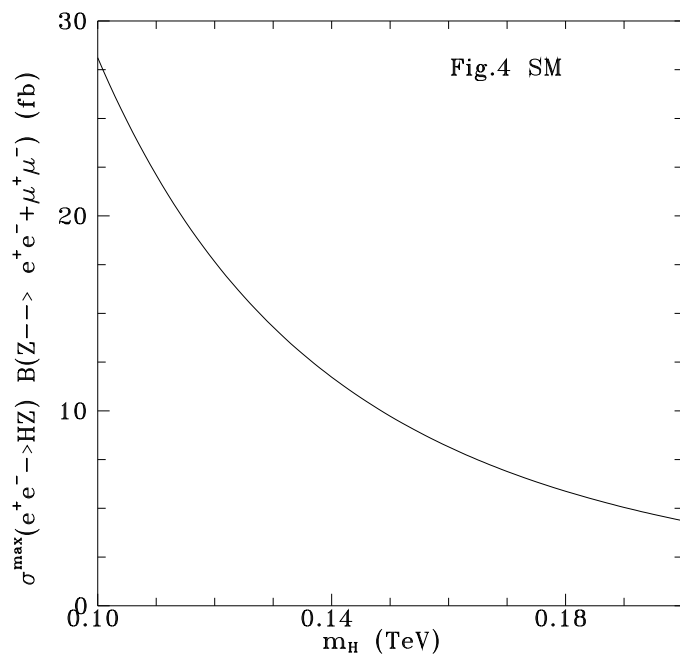


Figure 4: Maximal  $e^+ e^- \rightarrow HZ$  cross section versus  $m_H$ .

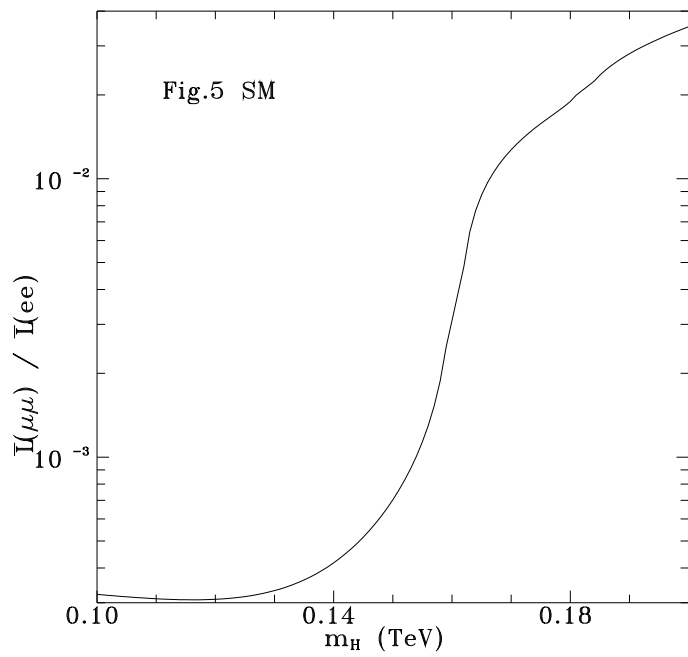


Figure 5: Ratio  $\bar{L}(\mu\mu)/\bar{L}(ee)$  required to get the same number of events in  $\mu^+\mu^- \rightarrow H$  and in  $e^+e^- \rightarrow HZ$ , versus  $m_H$ .

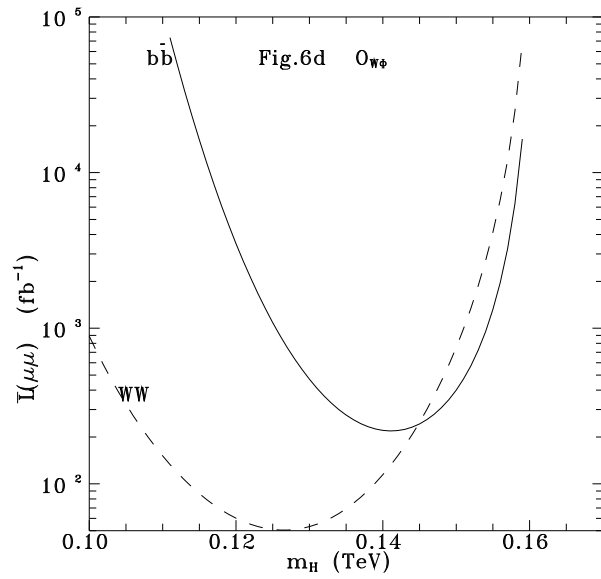
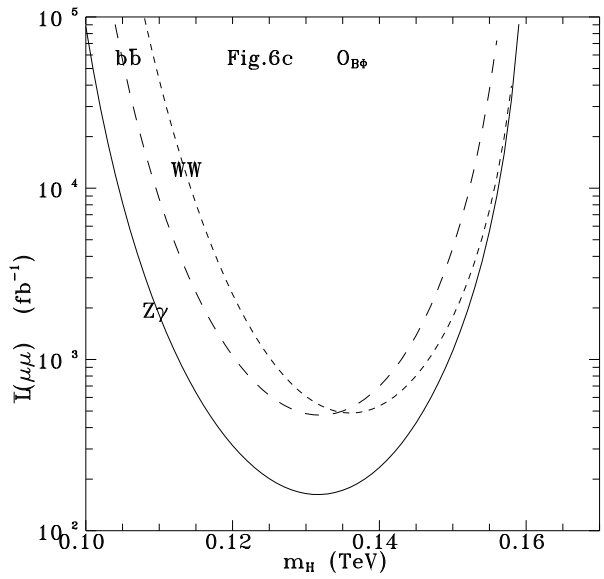
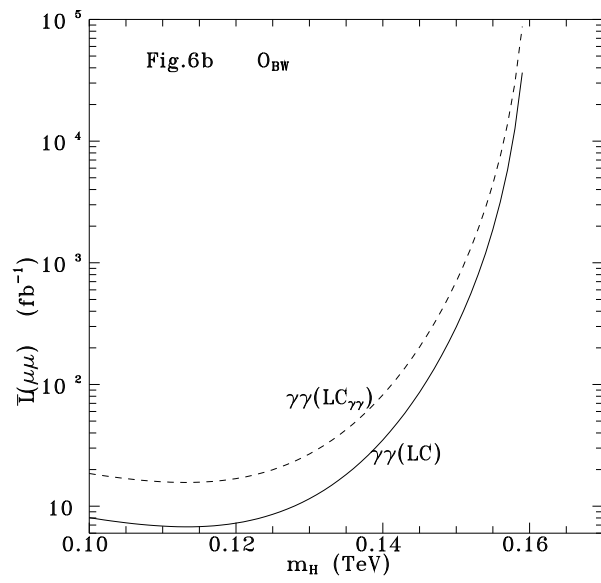
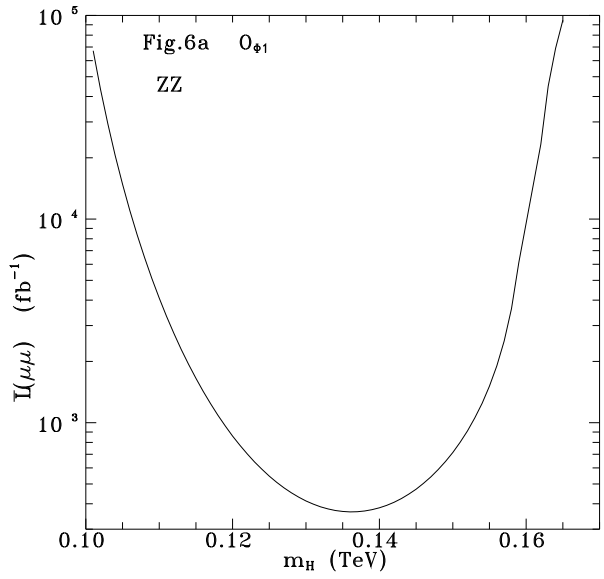


Figure 6:  $\mu^+ \mu^-$  luminosity needed to improve the constraint on operator  $\mathcal{O}_{\Phi 1}$  (a),  $\mathcal{O}_{BW}$  (b),  $\mathcal{O}_{B\Phi}$  (c),  $\mathcal{O}_{W\Phi}$  (d).

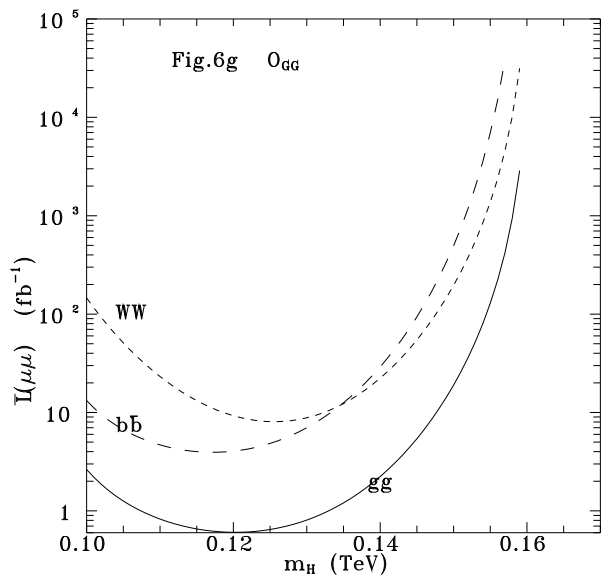
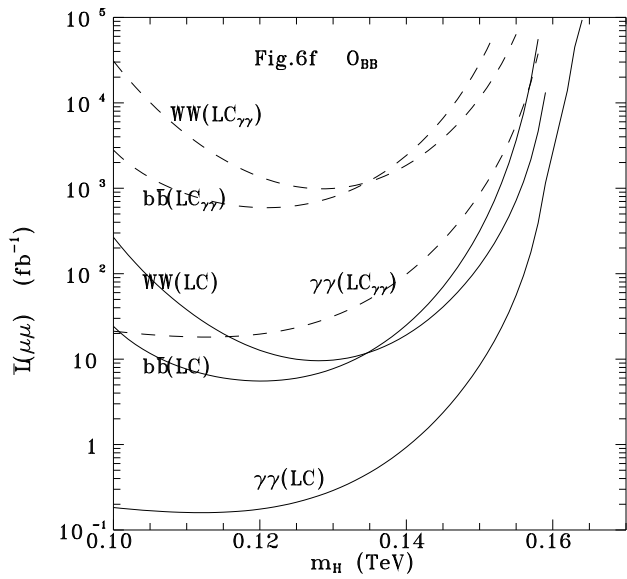
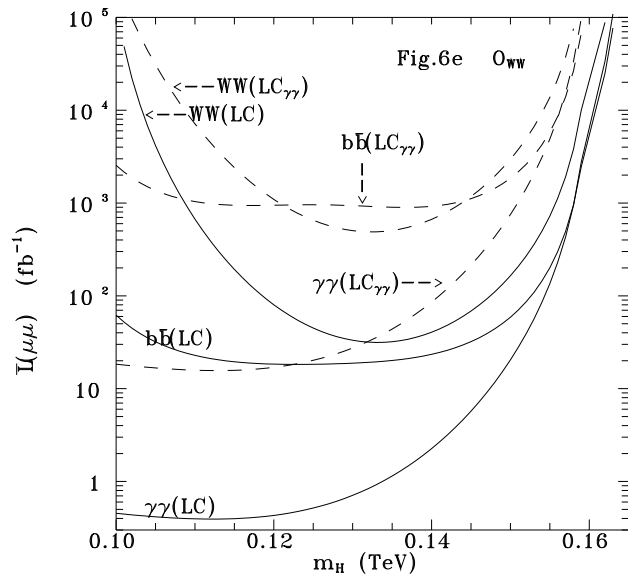


Figure 6:  $\mu^+ \mu^-$  luminosity needed to improve the constraint on operator  $\mathcal{O}_{WW}$  (e),  $\mathcal{O}_{BB}$  (f),  $\mathcal{O}_{GG}$  (g).

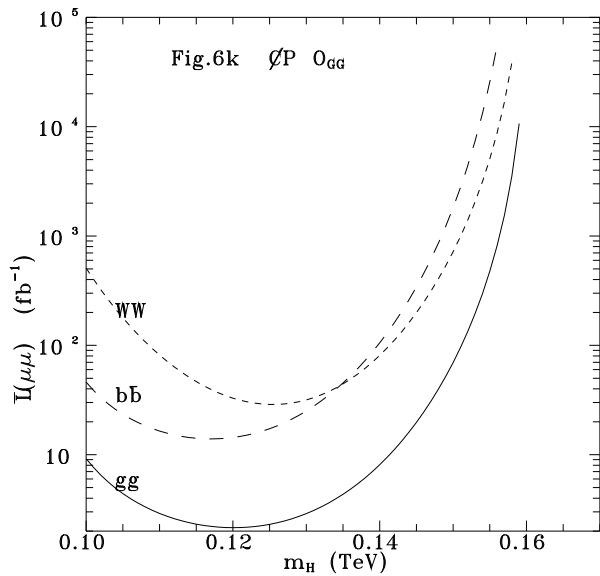
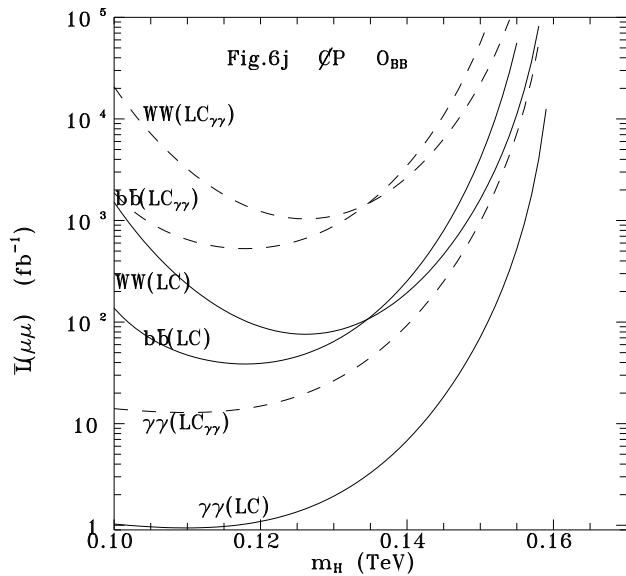
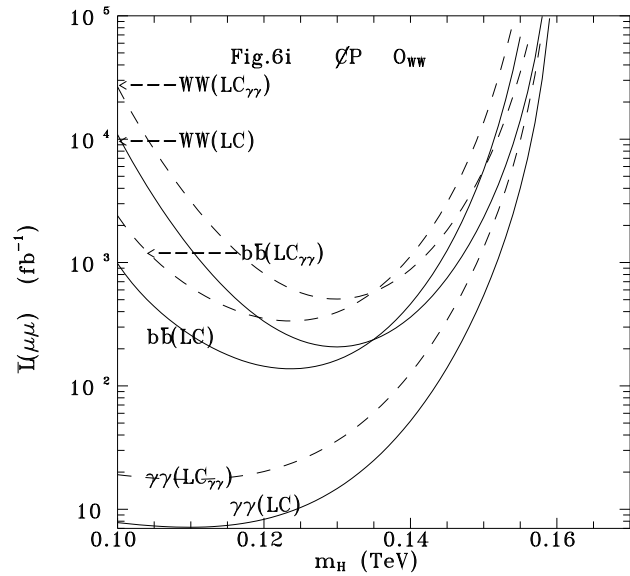
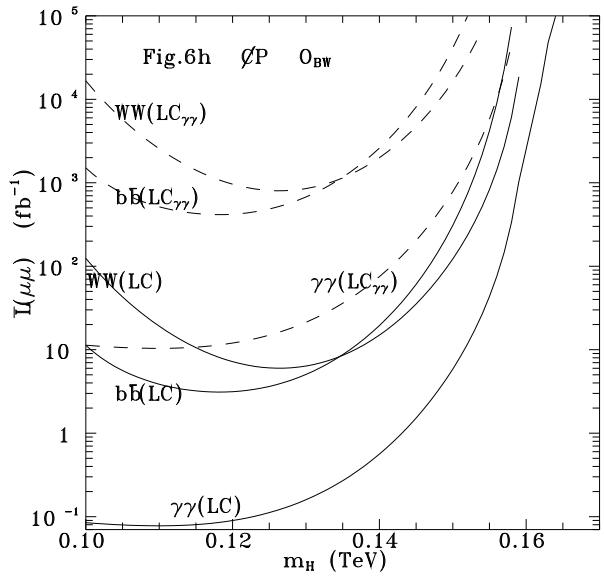


Figure 6:  $\mu^+ \mu^-$  luminosity needed to improve the constraint on operator  $\tilde{\mathcal{O}}_{BW}$  (h),  $\tilde{\mathcal{O}}_{WW}$  (i),  $\tilde{\mathcal{O}}_{BB}$  (j),  $\tilde{\mathcal{O}}_{GG}$  (k).

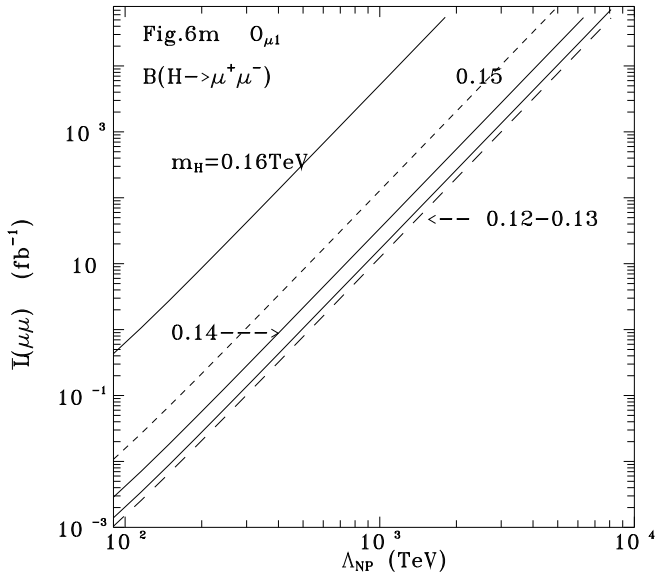
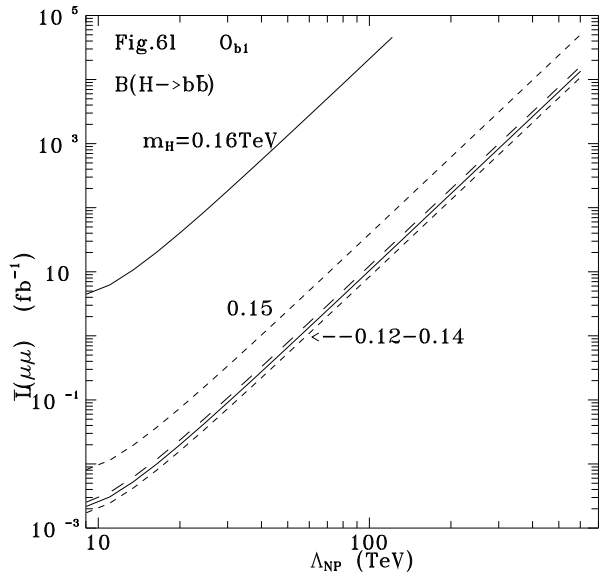


Figure 6:  $\mu^+ \mu^-$  luminosity needed to improve the constraint on operator  $\mathcal{O}_{b1}$  (l),  $\mathcal{O}_{\mu 1}$  (m).

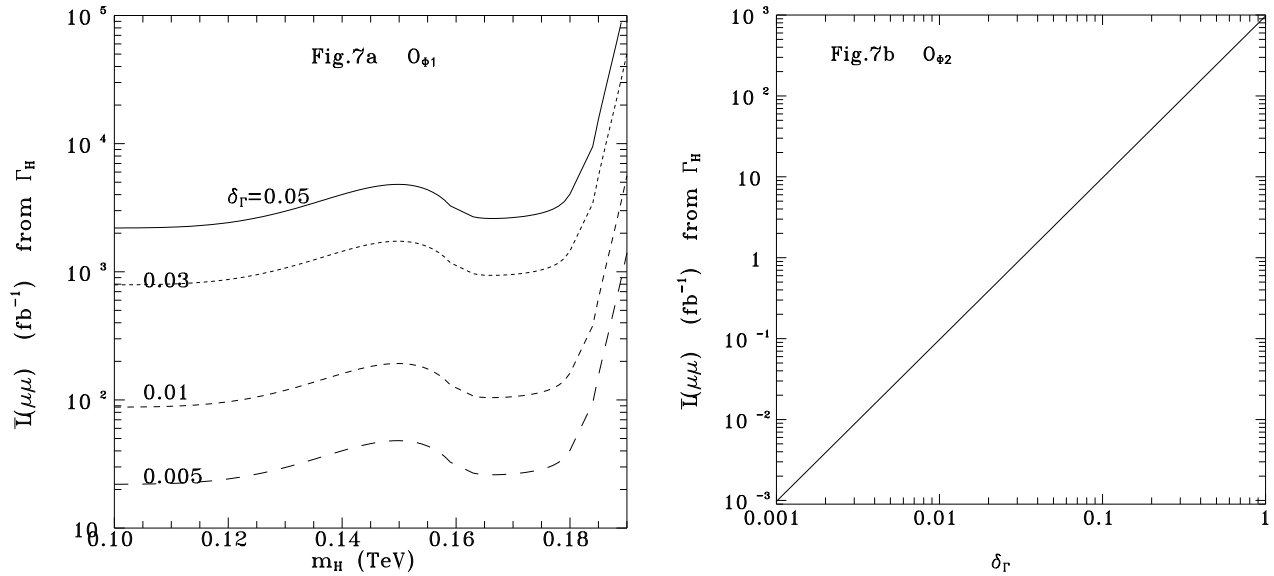


Figure 7:  $\mu^+\mu^-$  luminosity needed to improve the constraint on operator  $\mathcal{O}_{\Phi 1}$  (a),  $\mathcal{O}_{\Phi 2}$  (b), when the total width is measured with a relative accuracy parameter  $\delta_\Gamma$  as indicated.

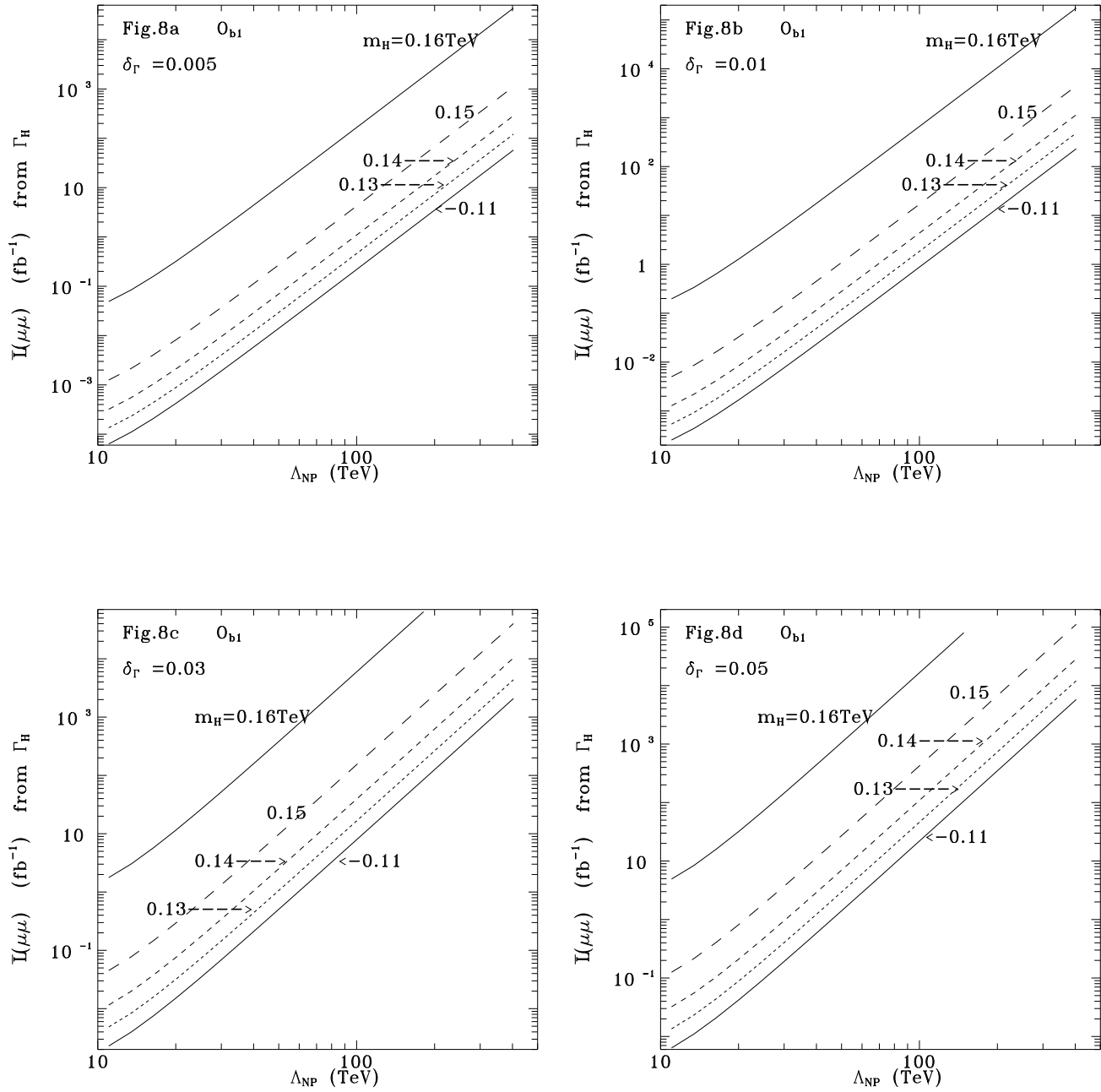


Figure 8:  $\mu^+ \mu^-$  luminosity needed to improve the constraint on operator  $\mathcal{O}_{b1}$  versus the fermionic scale  $\Lambda_{NP}$  for various values of  $m_H$  and for accuracies on the total width measurement,  $\delta_\Gamma = 0.005$  (a),  $\delta_\Gamma = 0.01$  (b),  $\delta_\Gamma = 0.03$  (c),  $\delta_\Gamma = 0.05$  (d).

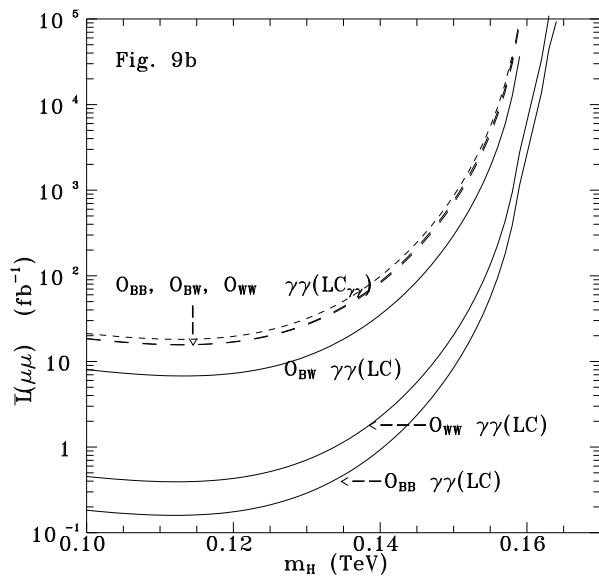
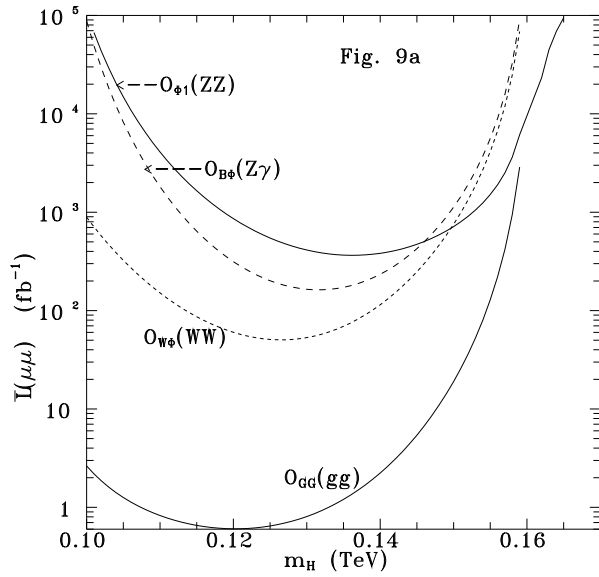


Figure 9:  $\mu^+ \mu^-$  luminosity needed to improve the constraints on the CP-conserving operators (only the most efficient channel is indicated).